Collection de notes internes de la Direction des Etudes et Recherches

Production d'énergie (hydraulique, thermique et nucléaire)

TESTS DE METHODES DE SIMULATION D'ECOULEMENTS TURBULENTS : RESULTATS D'ATELIERS POUR 5 CAS TESTS

TESTING OF CALCULATION METHODS FOR TURBULENT FLOWS : WORKSHOP RESULTS FOR 5 TEST CASES

98NB00004

EDF
Electricité de France

DIRECTION DES ÉTUDES ET RECHERCHES

SERVICE APPLICATIONS DE L'ELECTRICITE ET ENVIRONNEMENT

DÉPARTEMENT LABORATOIRE NATIONAL D'HYDRAULIQUE

EDF
Electricité de France

1998

RODI W.
BONNIN J.C.
BUCHAL T.
LAURENCE D.

TESTS DE METHODES DE SIMULATION D'ECOULEMENTS TURBULENTS : RESULTATS D'ATELIERS POUR 5 CAS TESTS

TESTING OF CALCULATION METHODS FOR TURBULENT FLOWS : WORKSHOP RESULTS FOR 5 TEST CASES

Pages : 36

98NB00004

Diffusion : J.-M. Lecœuvre
EDF-DER
Service IPN. Département PROVAL
1, avenue du Général-de-Gaulle
92141 Clamart Cedex

ISSN 1161-0611

EXECUTIVE SUMMARY :

Selected results of computations submitted to two ERCOFTAC Workshops on Turbulent Flow Calculations are presented, compared and discussed for 5 test cases. These are (i) Couette flow with plane and wavy fixed wall, (ii) 2D model hill flows, (iii) swirling boundary layer in conical diffuser, (iv) wing/body junction with separation and (v) developing flow in a curved rectangular duct.

Calculations were obtained with a wide variety of turbulence models including the standard κ-ε model with wall functions, various low-Reynolds-number versions of the κ-ε model, combinations with near-wall one-equation models in the two-layer approach, the RNG version of the κ-ε model, various non-linear versions, the k-ω model, various versions of Reynolds-stress, models, mostly with wall functions but also a low-Re version, an algebraic-stress model and for one test case also large-eddy simulations.

General conclusions on the performance of the various models were difficult to reach, partly because of the fact that quite different results were often obtained with nominally the same turbulence model by different contributors.

For the test cases considered, the more complex Reynolds-stress models and intermediate algebraic-stress and non-linear κ-ε models are not consistently better than the simpler linear eddy-viscosity models concerning the practically relevant mean quantities, but in some cases they were found to give superior predictions of the details of the turbulence quantities.

Testing of Calculation Methods for Turbulent Flows: Workshop Results for 5 Test Cases

W. Rodi, J.-Ch. Bonnin*, T. Buchal,
University of Karlsruhe,
Karlsruhe, Germany
and
D. Laurence
Electricité de France,
LNH, Chatou, France

1. INTRODUCTION

CFD is used more and more in the design process in virtually all fields of engineering involving fluid flow. For a successful application of CFD codes, their reliability and hence the quality of the calculations must be ascertained. Indeed, quality control is a key issue today. The quality of a CFD calculation is determined by the two components of the CFD software, namely the mathematical model for describing the flow processes by differential equations, and the numerical method used for solving these equations. As flows in practice are almost always turbulent, turbulence models for simulating the turbulent momentum, heat and mass transfer processes form an important part of the mathematical model. These models introduce a high degree of uncertainty in the accuray of CFD calculations even when the numerical errors can be kept under control. Due to the complex and diverse nature of the turbulence phenomena it seems unlikely that a universal turbulence model can be developed which yields reliable results for all flows. Hence, for quality control, it is important to calibrate and validate the CFD method for flow situations similar to those for which the method is to be used in practice.

The quality of the numerical method can be assessed by various methods calculating the numerical errors, grid refinement and application to problems for which exact analytical solutions are available. The quality of the turbulence model can only be assessed with the aid of reliable experimental data and recently (though only for simple flows at low Reynolds numbers) also with data obtained by direct numerical simulations. Hence, calculations of benchmark cases are indispensible for quality control of CFD methods for turbulent flows, and the availability of benchmark test cases based on reliable experimental data is very important. Moreover, the cases need to cover a wide range of flows occurring in engineering, to give an impression of likely width of applicability in practice. The provision of suitable data sets and the testing of CFD methods for a variety of flows of engineering interest are therefore key aspects of CFD validation.

In order to advance the creation of a data base and the testing of CFD methods and, in particular, the turbulence model components, a pan-European project on the topic "Data Validation and Comparison in Fluid Mechanics" was carried out, supported by the EC Programme SCIENCE and involving 7 partners of ERCOFTAC (European Research Community on Flow, Turbulence and Combustion). In this project, data (mainly experimental but also including DNS and some LES data) were collected and checked for their reliability and suitability as test cases; thereafter test cases were defined, and a data bank was created in which the data and test-case descriptions could be stored. Further, calculations of various of the test cases were carried out with a variety of turbulence models. The project work has yielded data for over 70 flows which are now stored in the ERCOFTAC data bank (Voke, 1996), and 15 well documented test cases were set up. At the end of the project, 5 cases were selected and offered to the general CFD community to calculate them and submit results to be presented at an ERCOFTAC workshop. This workshop entitled "Data Bases and Testing of Calculation Methods for Turbulent Flows" took place in Karlsruhe from April 3 to 7, 1995 and was the

* present address: VALTTEC, Futuropolis 6, F-86360 Chasseneuil, France

fourth in a series of ERCOFTAC/IAHR Workshops on Refined Flow Modelling. The test cases chosen are listed in Table 1, together with an overview on the submissions for each case. The cases were chosen such that they involved a range of different phenomena occurring in practical turbulent flows such as wall-bounded shear layers, separated flow, curvature effects, swirl, secondary motions, straight and curved boundaries, low and high Reynolds number situations. Further, the flows were also chosen to cover a range from fairly simple 2D cases to complex 3D flows with separation. Finally, it was felt to be essential to have well defined flow situations with sufficiently detailed data for testing of the calculation methods.

Thirty-six computor groups submitted altogether 99 results obtained with a wide variety of numerical methods and turbulence models which were compared with each other and with experimental data at the workshop. Some of the groups submitted results obtained with a range of turbulence models. The number of submissions for the individual cases are summarised in Table 1. Several errors and inconsistencies were detected during the workshop, and the contributors were invited to send corrected and updated results after the workshop to be included in the final workshop proceedings (Rodi et al 1995).

Test case 5 on the curved duct flow was issued again for the 5th ERCOFTAC/IAHR Workshop which took place in Chatou (near Paris) during April 25 - 26, 1996. 10 groups (all different from those who submitted results for the Karlsruhe Workshop) submitted altogether 25 different results for this case.

The purpose of the present paper is to provide a summary of the updated and corrected results submitted for the Karlsruhe Workshop, and for case 5, also for the subsequent workshop hosted by EDF-LNH in Paris. We discuss and interpret the results and draw conclusions so far as is possible. Of course, only a few samples of the many results can be included here. All results can be found in the workshop proceedings (Rodi et al 1995, Dauthieu et al 1996) where they are, however, compiled without any discussion.

Table 1: Test cases and overview on submissions

Case	Flow	Contri-butions	Groups	Turbulence Models
1	Couette flow with plane and wavy fixed wall	16	8	12
2	2D model hill flows	56	20	23
3	Swirling boundary layer in conical diffuser	13	8	11
4	Wing/body junction with separation	8	7	6
5	Developing flow in a curved rectangular duct	7+25*	5+10*	17

* submissions to Paris workshop

2. SUMMARY OF CALCULATION METHODS USED

In the workshop proceedings, the numerical methods and turbulence models used by each group are described in some detail, and they are summarised for each test case in tables, giving also the number of grid points/cells used. Here only a brief summary on the range of methods can be given.

As for the numerical solution procedures, most contributors employed finite-volume methods with collocated or staggered grids and SIMPLE-type algorithms for pressure-velocity coupling. Some methods were basically for compressible flows and employed the artificial compressibility method. Three finite-volume methods used unstructured grids. A wide variety of convection schemes was employed including upwind differencing and various blendings of upwind and central differencing, skew upwind differencing, higher-order upwind differencing, QUICK, TVD and MUSCLE schemes. 7 groups performed their calculations with finite-element methods and employed mostly streamline upwinding, but one scheme used the characteristics method for treating convection. In some finite-volume and finite-element methods employing the central differencing scheme, artificial dissipation/viscosity was introduced to ensure stability. Eight groups employed commercial CFD codes (altogether 4 different codes); 2 of these groups were the code vendors themselves while the others

had acquired the commercial codes. Some of the groups performed calculations with different grids and checked on the grid independence of their solutions, but in many cases only one grid was employed. The numerical accuracy of the various contributions is difficult to judge, but it can perhaps be speculated that the numerical errors were smallest in the Couette flow and swirling diffuser flow cases and generally larger in the flows with separation and the more complex 3D cases, especially when lower-order convection schemes were used.

The results submitted to the workshops were obtained with a wide variety of turbulence models, including the standard k-ε model with wall functions, a larger number of low-Reynolds-number versions of the k-ε model, a combination with a near-wall one-equation model in the two-layer approach, the RNG version of the k-ε model, various non-linear versions, the k-ω model, various versions of Reynolds-stress models, mostly with wall functions but also a low-Re version due to Launder & Shima (1989), an algebraic-stress model and finally also large-eddy simulations. An overview of the turbulence models used for each test case will be given when this is discussed in the next section.

3. TEST CASE CALCULATIONS

In this section, for each test case separately the case is introduced briefly, some sample results are presented and the general observations from all the results are summarised.

3.1 Test Case 1: Couette Flow with Plane and Wavy Fixed Wall

Three subcases were considered which are illustrated in Fig. 1. In cases A and B the walls were plane and the flow developed from channel flow between two fixed walls to Couette flow between a fixed and a moving wall. The difference between cases A and B is the Reynolds number. Experimental results due to Corenflos et al. (1993) are availabe for Re = 3000 and 5000, and for the lower Reynolds number, DNS data are available from Kuroda et al. (1993). In case C the upper fixed wall is wavy and periodic and the measurements at Re = 4000 (based on average height) are due to Nakabayashi et al. (1991).

Case 1A

This case is characterised by a fairly low Reynolds number (Re = 3000) and the channel flow develops from an initial state of pure Poiseuille flow to a semi Couette flow obtained by moving wall such that the mean velocity has a zero gradient at this wall. There is no shear and hence also no turbulent energy production near this wall. Because of the low Reynolds number, wall functions could not be used and all calculations were done by resolving the viscous near-wall layer. Calculations for developing flow (sample results see Fig. 2) were started at x/h = -7.9 with profiles obtained from a developed channel flow calculation. Results are non-dimensionalized by the bulk velocity U_b. Here the well known deficiency of the Launder-Sharma (1974) low-Re k-ε model shows up already, namely that the near-wall peak in turbulence intensity is severely underpredicted (not only due to the isotropic reditribution of k between normal components). The HJH*-Reynolds-stress model nearly gives the correct peak while the k-ω-model results of the U. of Concorde are intermediate. The underprediction of the turbulence intensity with the Launder-Sharma model continues near the upper wall to the developed Couette-flow state while near the moving wall the intensity is fairly well predicted. The RSM predicts the development at all stations fairly well while the k-ω model is initially also low near the upper, fixed wall. All models reproduce quite well the development of the mean-velocity profile from the symmetric developed channel flow profile to the strongly asymmetric Couette-flow profile with zero gradient at the moving wall. The development of the wall shear stress (not shown) along the fixed wall shows somewhat too high values in the downstream Couette-flow region for all models.

* Hanjalic´- Jakirdic´- Hadzic´ (1995)

For the developed Couette-flow region, sample results for U, $\overline{uv}$ and k are shown in Fig. 3, where they are compared with the experimental and DNS data: The experimental and DNS profiles of velocity and kinetic energy agree fairly well near the upper fixed wall, while there are some small differences near the lower moving wall. The shear-stress peak near the upper fixed wall is somewhat higher in the DNS calculations than in the experiments. The velocity profile is quite well predicted by all models; the differences are no larger than those between experimental and DNS results. Concerning the kinetic energy profile, the Launder-Sharma (LS) low-Re k-ε model and the two-layer model using the Norris-Reynolds (1975) one-equation model near the wall exhibit the known deficiency of underpredicting the k-peak in the shear layer. The two k-ω models show conflicting results in this respect, while using the Chien (1982) low-Re k-ε model or the RMM* one-equation model near the wall brings the peak close to the experimental and DNS values. Most Reynolds-stress models are also satisfactory in this respect. In the lower region near the moving wall, all models predict the k-profile reasonably well. The shear-stress distribution is generally quite well reproduced, with some results being a bit high (especially the U. Concorde k-ω predictions) and others being a little low. The individual normal stress components are predicted quite well by the Reynolds-stress models except for the UMIST models which show considerable discontinuities at the location switching from the stress-equation to the near-wall two-equation model used. The distribution of the dissipation rate ε near the walls is not well reproduced except for the Yang-Shih (1993) low-Re k-ε model and two RSM: HJH and LRR** with elliptic relaxation near the wall, which get the correct trend.

Case 1B

In this case with a somewhat higher Reynolds number (Re = 5000) the Couette flow has nearly an antisymmetric velocity distribution with velocity gradient and shear stress at the lower moving wall so that in this case there is a shear layer and turbulence production near this wall. In the developing flow region, similar remarks apply as made for case 1A, but the Launder-Sharma model (LS) now underpredicts the turbulence intensity peak also near the lower moving wall, leading further downstream to a too low intensity across the whole channel. The HJH-RSM simulates the development of the intensity profile fairly well at all stations. The development of the velocity profile is again well reproduced by all models, and so is the distribution of the wall shear stress along the fixed wall.

For the developed state of the flow for which sample results are shown in Fig. 4, the velocity distribution is quite well predicted by all models with a tendency of being a little low near the lower moving wall. In contrast to the experimental results which show pronounced peaks of k near the two walls, many models, among them most of the k-ε-based models predict a fairly uniform distribution of k across the channel. Only the Yang-Shih (1993) model yields pronounced peaks near the wall but also an excessive level in the centre region (the calculations of the same group with the LS version agree with the LS-model results of U.Delft). The U. Concorde k-ω model shows a similar behaviour and so do most of the Reynolds-stress models. The more sophisticated non-linear UMIST models do not cure the problem and yield again a fairly uniform distribution. They again also have a discontinous behaviour of the u- and v-components of the normal Reynolds stresses at the location of switching from the near-wall two-equation model to the stress-equation model in the main channel region. The other Reynolds-stress models predict reasonably well the distributions of the individual stress components, with somewhat too high levels of $\overline{uu}$ and $\overline{ww}$ in the channel centre. The total shear stress should be in developed Couette flow. The measured turbulent shear stress is not entirely uniform, having a small peak near the lower wall, which indicates that the flow was not fully developed in the experiments. The level of the calculated shear stress is higher than the measured one for all models. This discrepancy and also the generally higher predicted k-level in the channel centre, could to a large extent, be due to the fact that the flow was not fully developed in the experiment.

* Rodi, Mansour, Michelassi (1993)
** Launder, Reece, Rodi (1975)

Case 1C

This case with a wavy fixed upper wall had periodic conditions, and only one section covering one wave length was simulated and compared with the measurements. Inflow conditions did not have to be specified in this case which was hence independent of such conditions. The wavy wall induces an alternating streamwise pressure gradient, but this is not large enough to cause separation. Results have been obtained with the Launder-Sharma low-Re k-ε model, a two-layer model with the Norris-Reynolds one-equation model near the wall and the low-Re HJH Reynolds-stress model; profiles of U and $\overline{uu}$ at the location of smallest and largest channel width are shown in Fig. 5. The velocity profile is generally well predicted by all models, the velocity being slightly low in the centre part of the channel at x/L = 0.5. The distribution of the fluctuating velocity $\overline{uu}$ is generally well predicted by the Reynolds-stress model except that it is somewhat too high in the middle part of the channel and near the lower moving wall at the station with the largest channel cross section. The Launder-Sharma model predictions for the turbulence intensity are too low as discussed before.

Test Case 2: 2D Model Hill Flows

This case concerns the flow over 2D model hills mounted on the bottom wall of a plane channel. The experiments are due to Almeida et al. (1993) who provided the data for the two subcases: case A concerns the flow over a single hill and case B the flow over a series of consecutive hills with the same geometry. The channel height is 170 mm and the maximum height of each hill h_{max} = 28 mm and the length 108 mm. In the case of consecutive hills, the space between each hill is 4.5 h_{max}. The Reynolds number based on h_{max} and the channel centre-line velocity (upstream of the hill) is 60,000. The hills were placed 6 m (35 channel heights) downstream of the channel inlet and measurements obtained there in the absence of hills indicate a fully developed channel flow. The measurements were taken in the vertical centre-plane of the tunnel, but since this was only 200 mm wide (compared to the height of 170 mm), some deviations from two-dimensionality of the flow in this plane cannot be ruled out even though this was assumed in the calculations.

Case 2A

The flow over a single hill is considered here. As the opposite channel wall is 6 hill heights from the bottom wall, it has relatively little influence on the flow over the hill. A fairly large recirculation zone having a length of 4.4 hill heights develops. The calculations were started about 3.6 hill heights upstream of the hill centre using the developed channel flow measurements as inflow conditions; however, the ε-distribution was estimated by the individual computors and differed in some cases from what was used by the majority (the best approach being a preliminary channel flow caculation).

Altogether 38 different results were submitted. In the proceedings, they are plotted in 6 different groups according to the model type used. Of course, not all the results can be discussed and few can be presented here - only the more general trends can be given.

Streamlines

The streamlines give a good impression of the flow field and in particular on the separation and reattachment point and hence the length of the separation region. Fig. 6 compares the streamlines of 9 calculations with the measured ones. 6 computor groups submitted results obtained with the standard k-ε model using standard wall functions. Of these, 5 are reasonably close concerning the streamlines, with the separation predicted slightly too late and reattachment considerably too early so that the separation zone is too short by 25 to 40%. One calculation (U. Chalmers) yielded a much smaller separation region. A similar result was obtained by this group when using a Reynolds-stress model with wall functions. Reasons for this difference from the other calculations could not be determined with any certainty. Since the group obtained considerably larger

separation regions when resolving the near-wall region in one way or another, in agreement with calculations of others, the reason was thought to be in the code-specific treatment of the wall functions (these being nominally the same as in other calculations).

Some groups used the standard k-ε model with non-standard wall functions. Three of these calculations produced a recirculation zone that is smaller than when the standard wall functions are used while two produce a larger separation region, the latter being in fairly good agreement with the experiments. The use of the RNG version of the k-ε model also produces a larger separation region, which is in fact too large. Results obtained with two-layer models combining the standard k-ε model with various one-equation models near the wall yielded generally good agreement among the various calculations and come fairly close to the experimental picture. It should be noted that all calculations from the Florence group assumed a symmetry plane as the upper boundary instead of a wall and hence the results in the upper region are very different. When the RNG k-ε model is combined with a one-equation near-wall model, the recirculation length is too large. Four different low-Re k-ε models were used which give results similar to those obtained with the two-layer models, agreeing fairly well among each other and with the experiments. Only the Lam-Bremhorst version produces a too long separation zone. The conclusion that can be drawn here is that the prediction of the separation zone can vary significantly with the type of wall function implementation, and of course influences the size of the recirculation bubble. A low Re near-wall treatment.

Two results were obtained with non-linear k-ε models; the Shih-Zhu-Lumley (1994) version produces a recirculation zone smaller than the standard k-ε model while Speziale´s (1987) version gives realistic streamlines. A clear result is that the four calculations using the k-ω model agree very well among each other concerning the streamlines and predict a recirculation region which is too thick and about 35% too long.

As was mentioned already, the U. Chalmers Reynolds-stress model calculations with wall functions yield far too small recirculation zones but when this group resolves the near-wall region it produced the same result as obtained by U. Delft with the Launder, Reece and Rodi (1975) model together with wall functions, showing again the strong effect of the specific implementation of wall functions. With RSM, the separation zone is predicted longer than with the k-ε model but still somewhat shorter than experimentally observed. When the Gibson-Launder (1978) Reynolds-stress model is used (i.e. adding « wall echo terms »), the recirculation length is overpredicted (either with wall functions or with a one-equation near-wall model).

Profiles

Some sample profiles of U, V, k and $\overline{uv}$ are given in Fig. 7 for 3 streamwise locations. Approaching the hill crest and on top of the hill, the standard k-ε models with standard wall functions predict an unrealistic peak in U-velocity near the hill wall and excessive kinetic energy k and shear stress $\overline{uv}$, with the largest scatter in $\overline{uv}$ among the various results. Results of the group using non-standard wall functions or the RNG version of the k-ε model show similar trends, but there are larger differences between them, with some versions producing very high k-peaks near the wall. The two-layer models behave very similarly to the standard k-ε model; but the U-peak is not as strong, and most models predict a fairly good V-distribution over the hill top. The U-distribution obtained with the two-layer RNG model does not have the excessive peak near the wall. Most low-Re k-ε models do not show much difference to the standard k-ε model predictions in the region considered. The k-ω models produce less of a U-peak near the hill wall and also lower, more realistic shear-stress values, but too high tranverse velocity V over the top. Finally, the Reynolds-stress models yield just as excessive U-values near the wall as does the k-ε model but they do fairly well in terms of k and and $\overline{uv}$ profiles upstream of the crest and on top of the hill.

In the lee of the hill, encompassing the recirculation region, the development of the velocity profiles is of course closely related to the size of the separation region, i.e. the more realistic the size of this region is

predicted, the more realistic are also the velocity profiles, particularly in the reattachment region. All models underpredict the level of k and $\overline{uv}$ in the separated shear layer (if one can trust the measurements which show higher values than other separated-shear-layer measurements reported in the literature) and the peak values produced by the various calculations using the k-ε model/standard-wall-function differ by a factor of two. There is less scatter among the various low-Re k-ε model results and also the k-ω model predictions remain closer together. The Reynolds-stress models produced generally rather lower values of k and $\overline{uv}$ than the k-ε model predictions.

Further downstream, after reattachment, the U-velocity distribution is predicted fairly well by most k-ε-based models, the peak being somewhat closer to the lower wall than in the experiments. Here the k-ω models and also some of the Reynolds-stress models develop larger differences. As the peaks in k and $\overline{uv}$ become lower further downstream, these levels are better picked up by most models. The standard k-ε model with wall functions still underpredicts the peaks at the downstream station. Some versions using non-standard wall functions and two-layer models as well as low-Re k-ε models get the levels there reasonably correct. On the other hand, the k-ω model produces excessive k- and $\overline{uv}$ -levels further downstream, while most Reynolds-stress models still underpredict the levels.

Case 2B

This case concerns the flow over a series of hills. Detailed measurements were carried out between the 7th and 8th hill (of a series of 10), and from the experimenters (Almeida, Durao, 1993) it appeared that the flow was developed and periodic in this region. Hence, in the test-case specification computors were advised to assume periodicity conditions. In most calculations for which results were submitted (17 entries, ranging from k-ε models to RSM and LES) such conditions were used. However, a number of contributors raised doubts about the flow being fully developed after the 7th hill and performed non-periodic calculations, either by calculating the flow over the full series of 8 hills starting with developed channel flow upstream of the first hill as in case 2A, or by consecutive hill-by-hill solutions covering only the domain between two hill tops, feeding in the converged exit profiles from the previous calculation into the next. The results of these non-periodic calculations (5 entries, including LES) will be considered separately.

As the measurements may not really have been in a periodic region, the results obtained from periodic calculations should be considered with some caution.

Streamlines

Streamlines of 3 periodic calculations and 4 non-periodic calculations are shown in Fig. 8. The periodic calculations using the standard k-ε model with wall functions give roughly the measured separation and reattachment and size and shape of the separation region in the valley. Only the results from U. Porto give too small a recirculation region. The RNG version of the k-ε model gives more or less the same streamlines as the standard k-ε model. When the near-wall region is resolved either by a low-Re k-ε model, by a two-layer model approach or by using the k-ω model, separation is predicted too early and reattachment too late so that the resulting separation zone is too large. Reynolds-stress models also generally produce a too large recirculation region. An exception is the cubic model from UMIST. The LES results also show a recirculation region in reasonable agreement with the experiments.

The non-periodic calculations obtained with the k-ε model and wall functions show generally good agreement with the experiments concerning the separation and reattachment points; the separation zone is perhaps a little too wide. On the other hand, the Reynolds-stress model of Launder, Reece and Rodi produces too long and too thick a recirculation zone and the non-periodic LES calculations show early separation.

Profiles

Some sample profiles of U and k at the crest and valley locations are presented in Fig. 9. The profiles at the crest of the hill are considered first. The experiments show a fairly high U-value near the hill wall, which is not picked up in most calculations. An exception are the periodic calculations of U. Porto using the standard and a curvature-modified version of the k-ε model and wall functions. In general, the periodic calculations give too low U-values over the entire lower half of the channel, with the Reynolds-stress models being even lower than the k-ε models. The U. Karlsruhe group report that a fairly large number of iterations was necessary in their periodic k-ε model calculations to obtain a fully converged solution. They presented results of calculations with 2000, 12000 and 30000 iterations, and there was a clear shift of the peak in the velocity profile towards the upper wall between 2000 and 12000 iterations, but hardly any further shift when the calculations were continued to 30000 iterations. The profile then agrees fairly well with some other calculations obtained by Comp. Dyn. with the RNG model and by DLR with the k-ω model as well as with some of the Reynolds-stress models and with the LES calculation. It should be mentioned that the latter exhibits an excessive value of the lateral velocity V near the hill wall.

The U-profiles from the non-periodic calculations are closer to the experimental profile; the results from R.C. Hokkei with the k-ε model and non-standard wall functions are closest to the measurements. The other results are reasonably close but U is not high enough near the hill wall. The Reynolds-stress model calculations from U. Delft are better than their k-ε model calculations. The LES results show strange high values in the upper half of the channel.

The k-profiles at the hill crest are considered next. There is much scatter in the various k-ε model results, and the Reynolds-stress models do not faithfully reproduce the shape of the profile. The periodic LES calculations produce far too high k-levels. On the other hand, the non-periodic LES calculations yield a fairly reasonable k-distribution, with k still being somewhat too high near the wall (the shear stress $\overline{uv}$ is also overpredicted by a factor of 2). The other non-periodic calculations produce generally too low k-levels near the hill wall, the RNG and the U. Delft Reynolds-stress model calculations being considerably lower than the k-ε model results. Similar remarks apply to the distribution of the shear stress $\overline{uv}$.

At the centre of the valley (Fig. 9b), there is now a small negative velocity near the lower wall and a monotonic decrease in U-velocity in the lower part of the channel. Most periodic calculations underpredict the U-velocity in this part (in the region where U is positive) and overpredict U in the upper part. The best agreement with experiments was obtained by non-periodic calculations which over the most part lie fairly close to each other; the U. Delft Reynolds-stress model gives stronger reverse flow near the lower wall, as could be expected from the larger separation bubble. Again, the LES result has a strange high U-value in the upper region. In all calculations, the observed V-peak in the valley is not picked up. The calculated V-peaks are considerably smaller than the observed one. The high values of k near the lower wall at the valley center are also not picked up by any of the calculations and the same remarks apply as given for case 2A. The differences between the various periodic calculations are similar to what was discussed before. The U. Porto calculation with the k-ε model and curvature correction give the highest k-levels. In the non-periodic calculations the LES results are highest while RNG and Reynolds-stress model calculations produce far too low k-levels near the wall. Similar remarks can be made about the shear stress $\overline{uv}$.

Moving uphill towards the next crest, the picture is similar near the lower wall, the agreement between calculations and measurements improves, and in fact most non-periodic calculations show fairly good agreement over the whole channel depth (LES being again too high in the upper region). It should be noted that some of the models predict the wrong sign of the lateral velocity V, which is however much smaller than the U-velocity. The observed peak in k is now lower near the wall and can be picked up by some of the

calculations, but better by k-ε models than by Reynolds-stress models. In the non-periodic calculations, the peak is severely underpredicted with the same differences as for the periodic calculations.

Test Case 3: Swirling boundary layer in conical diffuser

This case concerns swirling flow in a 20° conical diffuser (see Fig. 10) as measured by Clausen et al. (1993). The diffuser starts 100 mm downstream of the swirl generator which consists of a rotating cylinder with honeycomb screen. At the outlet (x = 510 mm), the air discharges into the atmosphere. At the entrance to the diffuser, the streamwise velocity was nearly uniform except in the boundary layer which has a thickness of about 10% of the radius. Outside the boundary layer the flow was in solid body rotation. The swirl was strong enough to prevent separation in the diffuser; it causes a reduction of the streamwise velocity on the axis but was not strong enough to provoke flow reversal there. The measured profiles at a location 25 mm (= 0.2R) upstream of the diffuser entrance were to be taken as inflow conditions for the calculations.

Results were obtained with the standard k-ε model (3 entries), the RNG version of this model, the Jones-Launder low-Re version, the k-ω model, two versions of a non-linear k-ε model, an ASM model and the Launder, Reece and Rodi (LRR) Reynolds-stress model (2 entries). Except for the low-Re k-ε and the k-ω model, wall functions were used in all cases. In Fig. 11, sample profiles of axial velocity U, swirl velocity W, turbulent kinetic energy k and the shear stresses $\overline{uv}$ and $\overline{vw}$ are presented for the 2 axial locations x = 0.1 m and x = 0.33 m. In some of the calculations, the measured k-distribution at the inflow boundary was not used as initial profile in the boundary layer, but different (mainly lower) distributions were used. The initial k-level in the k-ω model model calculation was far too high, causing excessive k- and $\overline{uv}$-levels also in the initial diffuser region. The low-Re k-ε model calculations (not shown in Fig. 11) also develop excessive levels of k and of the shear stresses $\overline{uv}$ and $\overline{vw}$, which persist throughout the whole diffuser. In particular, the large value of $\overline{vw}$ near the wall is strange and entirely unrealistic. Also, the swirl velocity in these calculations is somewhat higher than in the experiments at most stations, indicating that the swirl number was not exactly matched to the experiments. The ASM and Reynolds-stress model calculations of k and shear stresses are also initially all too high. The ASM and the RSM calculations from TH Aachen stay high all the way through the diffuser while the RSM calculations of EC Lyon fall below the experimental levels towards the outlet of the diffuser. There are hence considerable differences in the calculated turbulence quantities between the calculations using nominally the same LRR Reynolds-stress model. The best agreement concerning the turbulence quantities was obtained by U. Brussels with the standard k-ε model and two non-linear k-ε model versions. The Hirsch-Khodak version produces the better results and is in fact the only model that can simulate reasonably well the distribution of the $\overline{uw}$ stress (which has, however, no influence on the mean-velocity field). For the other turbulence quantities the standard k-ε model gives results equally close to the measurements.

The reduction in U-velocity in the center portion towards the outlet of the diffuser is underpredicted by most models. Only the low-Re k-ε model calculation produces nearly the correct reduction. This may have to do with the fact that, compared with the other calculations, this model yields higher swirl velocity and shear stresses which are, however, also higher than the experimentally observed values. The LRR calculation from Lyon also yields lower U-velocity in the center portion in better agreement with the measurements, but strangely this is associated with smaller shear stresses (significantly below the experimental levels) than in the other models. With these two exceptions, there is generally good agreement among the various predictions about the development of the U- and W-velocity profiles; only at the station closest to the outlet there is considerable spread, the k-ε model yielding too high U-velocity at the axis. The streamwise distribution of pressure in the diffuser is calculated well by all models. The various k-ε model calculations also produced reasonable distributions of the axial and circumferential wall shear stress, while some of the other models yield too high values.

Altogether it seems that the standard k-ε model with wall functions gives results in this case which, apart from an insufficient reduction in the centre-line velocity, are reasonable for all quantities that are of practical interest. More complex models do not seem to yield a marked improvement. It appears that the swirl is not strong enough in this case to show the superiority of Reynolds-stress models reported in the literature for swirling flows.

Test Case 4: Wing/Body Junction with Separation

This case concerns the turbulent flow around a cylindrical airfoil mounted on a flat ground plate (see Fig. 12) at Re = 115000 (based on wing maximum thickness T). The experiments are due to Devenport and Simpson (1990) and Fleming et al. (1993) who measured the static pressure distributions on the ground plate and wing wall and the streamwise and secondary flow velocities as well as the Reynolds stresses in several vertical planes. The boundary layer on the flat plate separates when it approaches the leading edge of the wing and a horse-shoe vortex is formed which sweeps around the wing in the junction corner (see Fig. 13). The recirculation region in front of the leading edge exhibits large-scale unsteadiness characterised by a bimodal velocity probability density distribution with intense turbulence production. Calculations were started at x = -18.24 T where the boundary layer on the ground plate corresponded to a zero-pressure-gradient 2D boundary layer. The profiles for the mean velocity U and the turbulent stresses $\overline{uu}$, $\overline{ww}$ and $\overline{uw}$ at this station were to be taken those measured on the symmetry plane. The non-measured stress, $\overline{vv}$, was to be estimated as $2\ \overline{ww}\ -\ \overline{uu}$. Because of symmetry, only half of the flow needed to be calculated and computors were asked to extend the calculation domain to z = 3.5 T and to y = 3 T where symmetry conditions should be applied. The outflow was to be placed sufficiently far downstream (x > 10 T) so that zero gradients may be assumed without influencing the flow near the wing.

For this three-dimensional case, 7 groups submitted results; 6 of them employed versions of the k-ε model and 1 the Launder, Reece and Rodi Reynolds-stress model. 5 of the groups used wall functions and 2 the two-layer approach. The number of grid points used ranged from 100,000 to 500,000.

All calculations reproduced reasonably well the pressure distributions on the ground plate and the wing. In Fig. 13a) velocity vectors and streamlines constructed from these as well as turbulent kinetic energy contours are given in the symmetry plane in front of the wing for 3 calculations (all using wall functions) together with the experimental results. It can be seen that the general flow picture is well captured by the various models but that the separation vortex is predicted too thin and, particularly so with the RSM, also too short. The experiment shows fairly high turbulent kinetic energy k in the vortex region with centre at x/T = -0.2. As was mentioned already, the high turbulence in this region results from the horse-shoe vortex oscillating in a bimodal manner. This aspect cannot be reproduced by the steady calculations using standard turbulence models shown here. The calculations, except those with the RNG version of the k-ε model, yield the maximum of k closer to the corner and also produce excessive k in the stagnation region in front of the leading edge. This is a well known problem with the standard k-ε model. The RSM using a standard wall-echo correction in the pressure-strain term also suffers from this, albeit to a lesser extent: the $\overline{uu}$-component is overpredicted by including the wall-echo correction (this was encountered in former Workshops, e.g. tube bundle crossflow or impinging jet, Craft & Launder (1991), provide an alternative treatement of the wall echo term). On the other hand, the RNG model does not seem to have this problem and yields the maximum of k correctly in the vortex core, but with a much smaller value than in the experiments.

When sweeping around the wing, the strength of the horse-shoe vortex is underpredicted by all models. At x/C = 0.18 the secondary flow is directed mainly outward due to the displacement effect of the wing; the horse-shoe-vortex motion is superimposed, but is difficult to detect. In the corners the flow goes diagonally

from the wing to the plate where it seems to "bounce off" at z/T = 0.09, indicating the extent of the horse-shoe vortex. Most computations show a more diffused picture of the horse-shoe vortex, particularly those that overpredict the k-levels in the stagnation region and give thereby rise to a thicker boundary layer on the wing. Hence the RSM and in particular the RNG model give the secondary motion in closest agreement with the measurements. The k-maximum is generally predicted too close to the wing. This trend continues further downstream and secondary velocity field and k-levels are shown in Fig. 13b) for a plane at x/C = 0.75. As before, in the experiment the extent of the horse-shoe structure can be detected by a relatively sharp kink in the secondary flow streamlines, now at z/T = 1.1. Again, in most computations the picture is more diffuse, and only RNG and RSM get a behaviour reasonably similar to the experiment. High k-levels were measured in the region of the kink, a feature only reproduced by the RSM while all the other models significantly undepredict the level of k. In the plane immediately downstream of the trailing edge of the wing (x/C = 1.05), size and strength of the vortex are also underpredicted. The turbulent kinetic energy, k, now has two maxima, one towards the outer edge of the vortex and the other in the wake behind the trailing edge; this feature is picked up by all models and best reproduced by the RSM while the RNG model now gives too low values of k.

In conclusion, although all computations captured qualitatively the general flow patterns, the sharpness of the predicted horse-shoe vortex is affected adversely by erroneous overprediction of turbulent energy in the wing stagnation region that is carried downstream. The RNG model does not seem to encounter this problem but underestimates *k* further downstream. Although the computations obtained with the RSM were performed with the coarsest mesh in the horse-shoe vortex region, the results are encouraging. It appears that the RSM would be consistently superior if calculations were done on a mesh as fine as with the other calculations. Another item for further investigation is whether time-dependent simulations could capture the bimodal aspect of the vortex structure.

Case 5: Developing Flow in a Curved Rectangular Duct

The flow through a 90^{o} bend of a rectangular duct is considered at Re = U_0H/ν = 224000. The width is H, the height 6 H, the radius of the inner curved wall is R_i = 3 H and the duct has a straight section of length 7.5 H upstream and of 25.5 H length downstream of the bend (see Fig. 14). Due to the high aspect ratio, the flow in the middle part of the duct away from the top and bottom walls is quasi two-dimensional, with the boundary layers subjected to strong streamwise curvature, the one on the inner convex wall stabilising and the one on the outer concave wall destabilising, exhibiting Görtler vortices. Near the top and bottom walls, the pressure-driven secondary motion develops first on the horizontal walls, then sweeps up along the inner vertical wall. Kim and Patel (1994) have carried out detailed measurements of the components of mean velocity and Reynolds stresses with a 5-hole pressure probe and two-sensor hot-wire probes as well as of the wall shear stress and wall static pressure distributions.

The calculations were started 4.5 H upstream of the bend where the detailed velocity and Reynolds-stress measurements were to be taken as inflow conditions. At this station, the velocity is uniform in the core; on the vertical walls the boundary layers are of flat-plate type with a momentum-thickness Reynolds number of 1650, a boundary-layer thickness of δ = 0.08 H and a friction coefficient of c_f = 0.0038. The wind tunnel contraction 3H upstream of this station generates pairs of counterrotating vortices near the top and bottom wall with the secondary motion about 5% of the axial velocity. This motion needed to be prescribed as part of the inflow conditions. The outflow boundary was to be placed at x > 30H so that zero gradients could be assumed.

For the Karlsruhe workshop, 5 groups submitted 7 results for this case obtained with various versions of the k-ε model, including non-linear and algebraic stress (ASM) variants and with the Gibson-Launder RSM. All models employed wall functions. For the Paris workshop, 10 (different) groups submitted altogether 25 results for this case. The turbulence models used include the standard k-ε model with wall functions, various low-Re k-ε models, two-layer k-ε models, various non-linear k-ε models, the k-ω model, and a variety of Reynolds-

stress models, mostly using wall functions, but also low-Re versions. Mostly 200000 - 300000 grid points were used, but with typically 50 - 60 grid points in the cross-flow directions, the resolution may not be high enough when low-Re versions of turbulence models are employed.

We first consider the three-dimensional flow that develops near the bottom (and analogously near the top) of the duct with the aid of secondary velocity vectors and contours of turbulent kinetic energy at 45^{o} in Fig. 15. The pressure gradient in the curved section drives low-momentum flow near the floor towards the left, inner wall, generating a large clockwise-rotating vortex. This motion enhances the vortex with clockwise rotation and annihilates that with anti-clockwise rotation of the initial pair generated by the wind tunnel contraction. This explains the apparently scrambled secondary velocities seen in Fig. 15. The fine-grid computations in which the initial vortex pair is well accounted for (e.g. EDF, U. Brussels, U. McGill and Chalm) show a consistent "clover leaf"-like structure with the initial clockwise-rotating vortex sitting on top of the pressure-driven boundary-layer motion. This picture is less clear in the experiments, possibly because of the lower resolution. As already indicated by the results at 45^{o} shown in Fig. 15, the secondary flow vectors at 75^{o} (not shown) reveal that the wall-jet type behaviour of the secondary flow on the inner wall is generally better reproduced by Reynolds-stress models than by eddy-viscosity models which yield a turning of this flow away from the wall much closer to the corner than observed in the experiments. The tongue of k penetrating in the experiments from the bottom wall into the core through the upward motion of the vortex pair is best predicted by the ASM and the cubic RSM.

Away from the top and bottom walls, the nearly 2D boundary layers on the inner and outer walls develop a strong asymmetry due to the different pressure gradients and curvatures prevailing: the boundary layer on the inner wall becomes thinner and k is reduced while on the outer wall it becomes thicker and k is increased due to the effect of concave curvature. This trend is simulated fairly well, as can also be seen from Fig. 17 showing examples of k-profiles at 45^{o}. There is in fact little difference between the various model types, and the figure reveals that the fairly high values of k measured near the outer wall with concave curvature are not reached by any model, including the RSM which is expected to account properly for curvature effects. These high levels may be due to Taylor-Görtler vortices, and the RSM calculations of TU Delft show instabilities which indicate that there is a tendency towards such vortices in these calculations. A careful time-dependent simulation (without a symmetry plane condition) would be required to check this point.

Fig. 16 shows the final development of the secondary motion 4.5 H downstream of the bend and the k contours 1H from the bend (not available at 4.5 H). Now the pressure-driven motion on the floor has pushed up the vortex along the left wall which terminates the jet-type flow on this wall. Underneath, in the experiment the clockwise vortex originating from the contraction is still visible. This structure has, however, vanished in the computations although there are some slight traces still visible in the GTech and UMIST results. Most computations now show a single vortex which is generally wider and located closer to the corner than in the experiments. Numerical diffusion now probably hides the effects of the turbulence models. The predicted k-contours all show a maximum in the region of the longitudinal vortex, in agreement with the measurements. On the outer wall there is now a wide region of high k, the extent of which is underpredicted by virtually all models but perhaps least so by the ASM. The level is also generally underpredicted and an explanation could be again that Taylor vortices may have been generated on the outer wall with concave curvature including some temporal instabilities counted as turbulence. The EDF and TU Delft calculations show such instabilities, but the mesh was probably not fine enough to properly resolve the longitudinal vortices.

The distribution of the friction coefficient c_f along the wall is shown for stations 15^{o} and d1 (0.5H downstream of the end of the bend) in Fig. 18. Upstream of the bend, the friction coefficient on the inner and outer wall is nearly the same and the level is roughly reproduced by most models, with a tendency of being a little high. Moving through the bend, c_f develops strong asymmetry between inner and outer wall, first

reaching higher values on the inner wall and at the end of the bend higher values on the outer wall. At 15°, the increase of c_f on the inner wall is captured fairly well by most models, probably because it is mostly due to the higher axial velocities there. Also, the eddy-viscosity models do a good job and are fairly close together, while there is a rather wide spread among the RSM. Near the floor, where the vortex pair induces a « W » shaped c_f profile, the agreement with the experiments is not so good. At the end of the bend, where the distribution of c_f has been reversed, none of the eddy-viscosity models show sufficient asymmetry while the RSM calculations of U.McGill and Chalm do a good job, but only the latter is correct at both sections. Here is some evidence that stress-equation models account better for the effect of curvature on turbulence than do eddy-viscosity models. When moving from the floor up the inside wall, the lower values of c_f between $s = 3.$ and $s = 2.$ associated with the wall-jet structure of the secondary motion is not predicted by any model. The isolevels of axial velocity show that this is a region of very thin boundary-layer thickness which is not entirely captured by the models. Finally, the sharp dip in c_f at $s = 2$ corresponds to the vortex structure at the end of the wall jet moving low-momentum fluid away from the wall. This phenomenon is reasonably well captured by most models.

Altogether, the results for this test case are not entirely conclusive. Certain stress-equation models reproduce some of the details better than eddy-viscosity models, but on the whole a clear-cut superiority is difficult to discern. The effect of spatial resolution must be investigated but this would require considerably finer meshes with more than 1 million grid points.

4. CONCLUSIONS

The good attendence of the workshops and the large number of results contributed have confirmed the importance of the issue of quality control in CFD and the considerable interest - also in industry - in test calculation exercises. The workshops have also shown that developers, vendors and users of CFD codes are prepared to participate in such exercises. The test cases ranged from fairly simple low-Reynolds-number channel-type flow to complex high-Reynolds-number 3D flows, covering a wide range of flow and turbulence phenomena. They were calculated with a wide variety of turbulence models with a perhaps somewhat bewildering number of different variants. The results shed some light on the performance of the various models but no clear picture emerged and general conclusions are difficult to reach, for reasons addressed below. However, some useful observations could be made which will now be summarised. In some of the test cases, the turbulence quantities were better predicted with the more complex Reynolds-stress and also algebraic-stress or non-linear eddy-viscosity models than with the linear eddy-viscosity models; a clear case here is the Couette flow where the eddy-viscosity models predict a too uniform distribution of the turbulent kinetic energy. Also, in stagnation regions where linear eddy-viscosity models produce excessive k-production, and when significant streamwise curvature effects on turbulence are present, RSM and ASM yield superior results, in the case of the curved channel flow also concerning the details of the secondary flow. However, for the test cases considered, the more complex models were not consistently better than the simpler linear eddy-viscosity models as far as the practically relevant mean-flow quantities are concerned. This is true also for the swirling diffuser flow which did not prove a particularly severe test case. In the single-hill flow, the prediction of the separation behaviour was improved when the near-wall region was resolved rather than treated by wall functions and also by moving to Reynolds-stress models, but this was not the case for the series of hills. It should also be noted that for most cases considered, entirely satisfactory agreement with experiments could not be achieved with any model.

The difficulty in reaching general and well supported conclusions is due to a number of reasons. One is the fact that the results obtained with nominally the same turbulence model were in many cases substantially different so that they were difficult to compare. The reasons for these differences could not be found out. Secondly, on closer examination, some of the experiments were not sufficiently close to the specified conditions, e.g. the Couette-flow case 1B was probably not fully developed and the periodic hill-flow case 2B

was not really periodic, nore maybe two-dimensional, in the experiments. Thirdly, the numerical resolution of the various calculations was sometimes quite different and in some cases not sufficient, especially for the 3D flows when the near-wall region was not treated by wall functions but with a low-Reynolds-number model. For future workshops and test-case exercises, the experiments must be scrutinized even more so that more reliable experimental target values are available. Further, accurate benchmark solutions must be obtained for the individual test cases, at least with some of the more standard models. Such solutions should help to spot any irregularities that may be caused by coding errors, numerical inaccuracies or incorrect specification of boundary conditions.

ACKNOWLEDGEMENTS

The Karlsruhe workshop was financially supported by COMETT II through UETP ERCOFTAC, COST, the University of Karlsruhe and EDF; the Paris workshop was sponsored by EDF and ERCOFTAC.

5. REFERENCES

Almeida, G.B., Durao, D.F.G. and Heitor, M.V., 1993. Wake flows behind two-dimensional model hills. *Exp. Thermal and Fluid Science*, **7**, 87-101.

Chien, K.Y., 1982. Predictions of channel and boundary-layer flow with a low-Reynolds-number turbulence model. *AIAA J.*, **20**, 33-38.

Clausen, P.D., Koh, S.G. and Wood, D.H., 1993. Measurements of a swirling turbulent boundary layer developing in a conical diffuser. *Exp. Thermal and Fluid Science*, **6**, 39.

Corenflos, K., Rida, S., Monnier, J.C., Dupont, P., Dang Tran, K. and Stanislas, M., 1993. Experimental and numerical study of a plane Couette-Poiseuille flow as a test case for turbulence modelling. in *Engineering Turbulence Modelling and Experiments II*, W. Rodi and F. Martelli eds., Elsevier Publ., 499-508.

Craft T.J., Launder B.E., 1991. Computations of Impinging Flows using Second Moment Closures, *8th Symp. Turb. Shear Flows, Munich.*

Dauthieu, I., Laurence, D. and Richoux, S., 1996. Proc. of 5th ERCOFTAC/IAHR Workshop on Refined Flow Modelling, Chatou (Paris), April 25-26, Electricité de France, Laboratoire Nationale d´Hydraulique.

Devenport, W.J. and Simpson, R.L., 1990. An experimental investigation of the flow past an idealised wing-body junction: preliminary data report, version 5. Report of Virginia Polytechnic Institute and State University.

Fleming, J.L., Simpson, R.L., Cowling, J.E. and Devenport, W.P., 1993. An experimental study of a turbulent wing-body junction and wake flow. *Exp. in Fluids*, **14**, 366.

Gibson, M.M. and Launder, B.E., 1978. Ground effect on pressure fluctuations in the atmospheric boundary layer. *J. Fluid Mech.*, **86**, 491-511.

Hanjalic´, K., Jakirlic´, S. and Hadzic´, I., 1995. Computation of oscillating turbulent flows at transitional Re numbers. in *Turbulent Shear Flows 9*, 323-342, eds. F. Durst et al., Springer, Berlin.

Kim, W.J. and Patel, V.C., 1994. Origin and decay of longitudinal vortices in developing flow in a curved rectangular duct. *J. Fluids Eng.*, **116**, 45-52.

Kuroda, A., Kasagi, N. and Hirata, M., 1993. Direct numerical simulation of turbulent plane Couette-Poiseuille flows: effect of mean shear on the near-wall turbulent structures. *Proc. Symp. on Turbulent Shear Flows 9*, Kyoto, Japan, 8-4-1.

Launder, B.E. and Sharma, B.I., 1989. Second momenent closure for the near wall sublayer: Developpment and application. *AIAA Journal*, **27**, 1319-1325.

Launder, B.E. and Shima, N., 1989. Application of the energy-dissipation model of turbulence to the calculation of flow near a spinning disc. *Let. Heat Mass Transfer*, **1**, 131-138.

Launder, B.E., Reece, G.J. and Rodi, W., 1975. Progress in the development of a Reynolds-stress turbulence closure. *J. Fluid Mech.*, **68**, 537-566.

Nakabayashi, K., Kitoh, O. and Iwata, H., 1991. Turbulent Couette-type flow with an alternating pressure gradient. *Proc. Symp. on Turbulent Shear Flows 8*, Munich, Poster I-13.

Norris, H.L. and Reynolds, W.C., 1975. Turbulent channel flow with a moving wavy boundary. Rept. No. FM-10, Stanford University, Dept. Mech. Eng.

Rodi, W., Bonnin, J.-C. and Buchal, T.. Proc. ERCOFTAC Workshop on Data Bases and Testing of Calculation Methods for Turbulent Flows, University of Karlsruhe, Institute for Hydromechanics, April 3-7, 1995, available on-line from: ftp://ftp-ifh.bau-verm.uni-karlsruhe.de/workshop/proceedings.

Rodi, W., Mansour, N.N. and Michelassi, V., 1993. One-equation near-wall modelling with the aid of direct simulation data. *J. Fluids Eng.*, **115**, 196-105.

Shih, T.-H., Zhu, J. and Lumley, J.L., 1994. A new Reynolds-stress algebraic equation model. NASA TM 10664.

Speziale, C.G., 1987. On non-linear k-l and k-ε models of turbulence. *J. Fluid Mech.*, **178**, 459-475.

Voke, P.R., 1996. The ERCOFTAC Fluid Dynamics Database. *ERCOFTAC Bulletin* No. **30**, 57.

Yang., Z. and Shih, T.-H., 1993. New time-scale based k-ε model for near-wall turbulence, *AIAA J.*, **31**, 1191-1198.

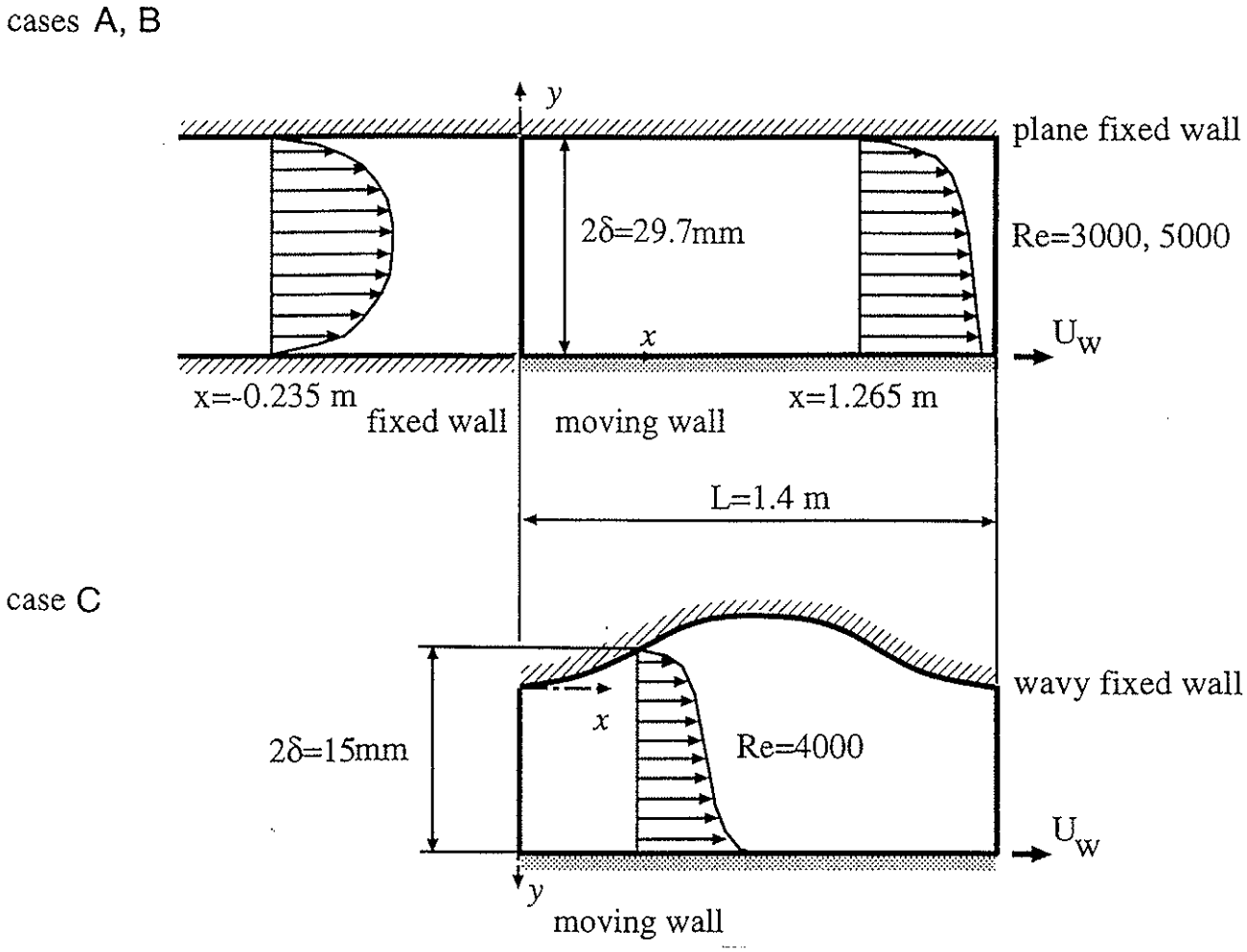

Fig. 1: Test case 1: Couette flow, flow configurations

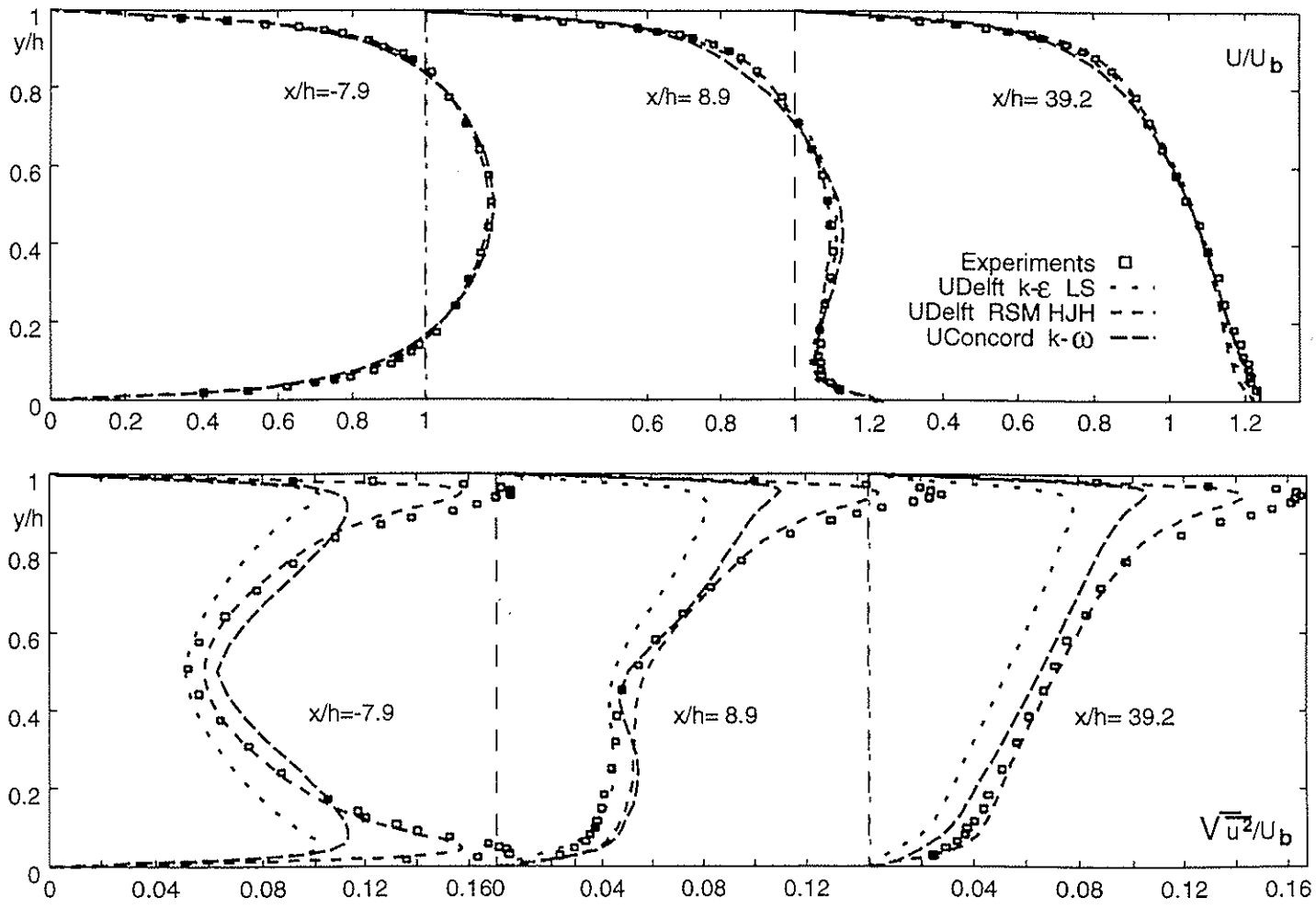

Fig. 2: Couette-flow test case 1A: development of profiles

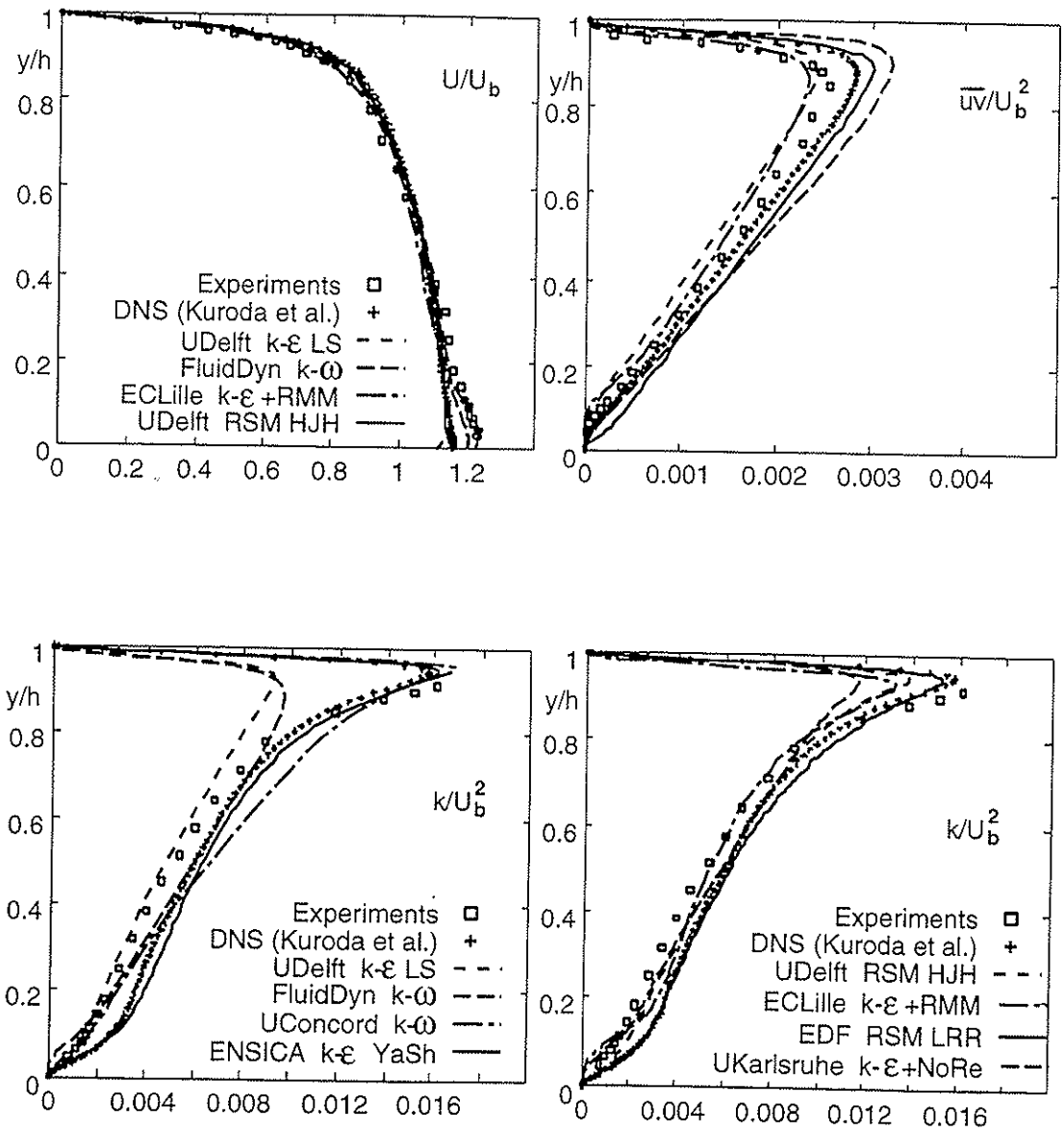

Fig. 3: Couette-flow test case 1A: developed profiles

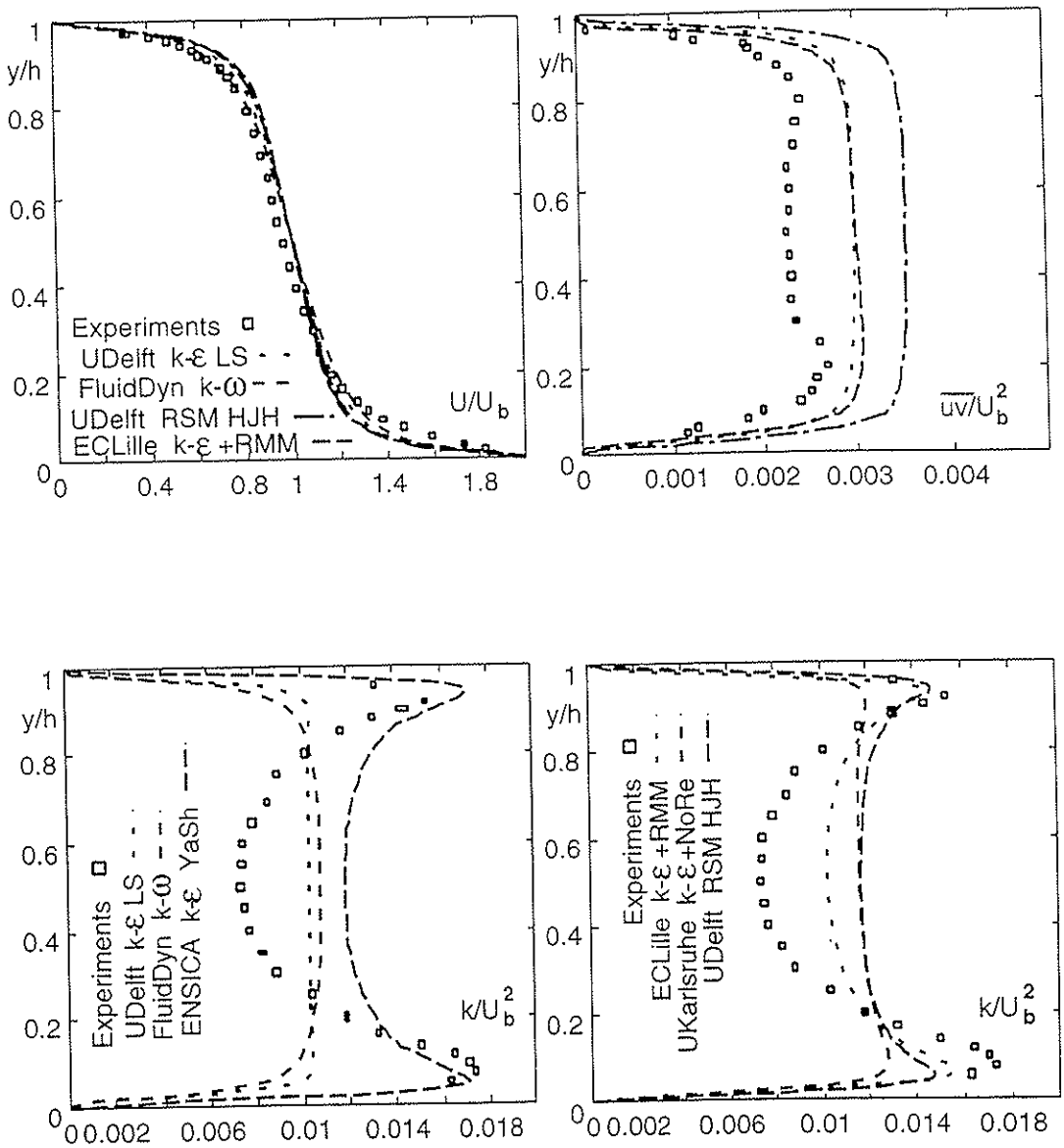

Fig. 4: Couette-flow test case 1B: developed profiles

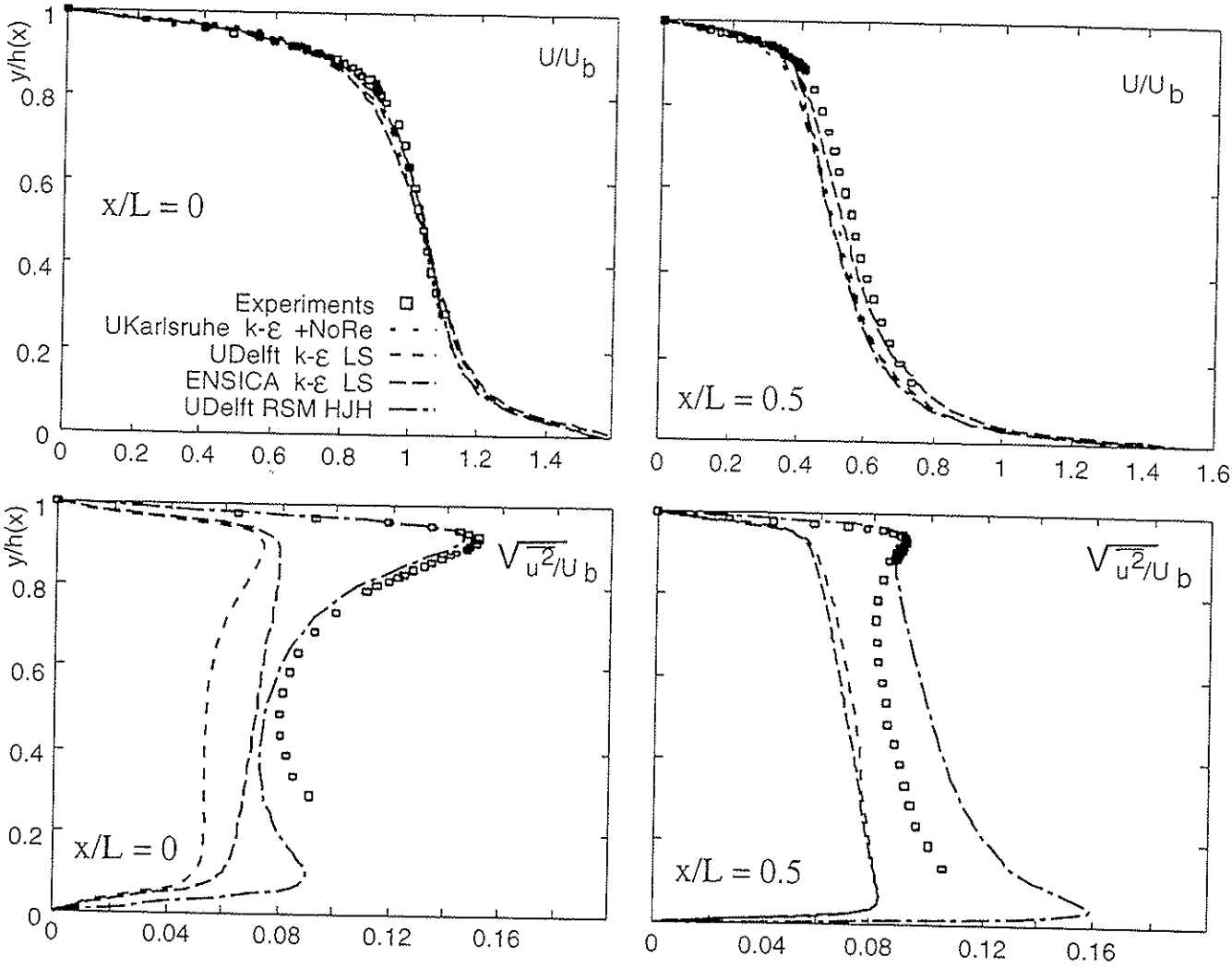

Fig. 5: Couette-flow test case 1C: profiles at location of lowest and highest point of wavy wall

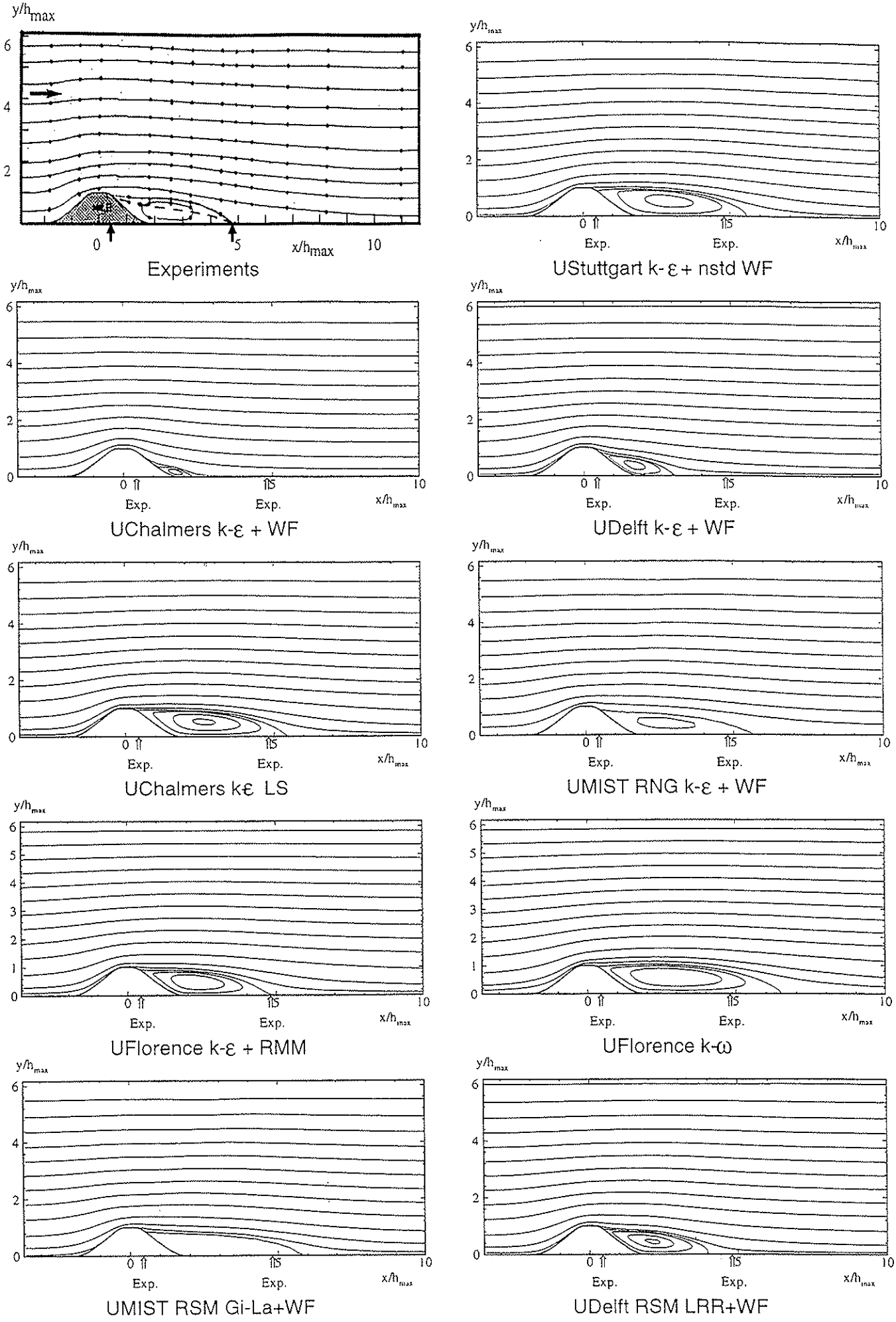

Fig. 6: Test case 2A: 2D single-hill flow; streamlines

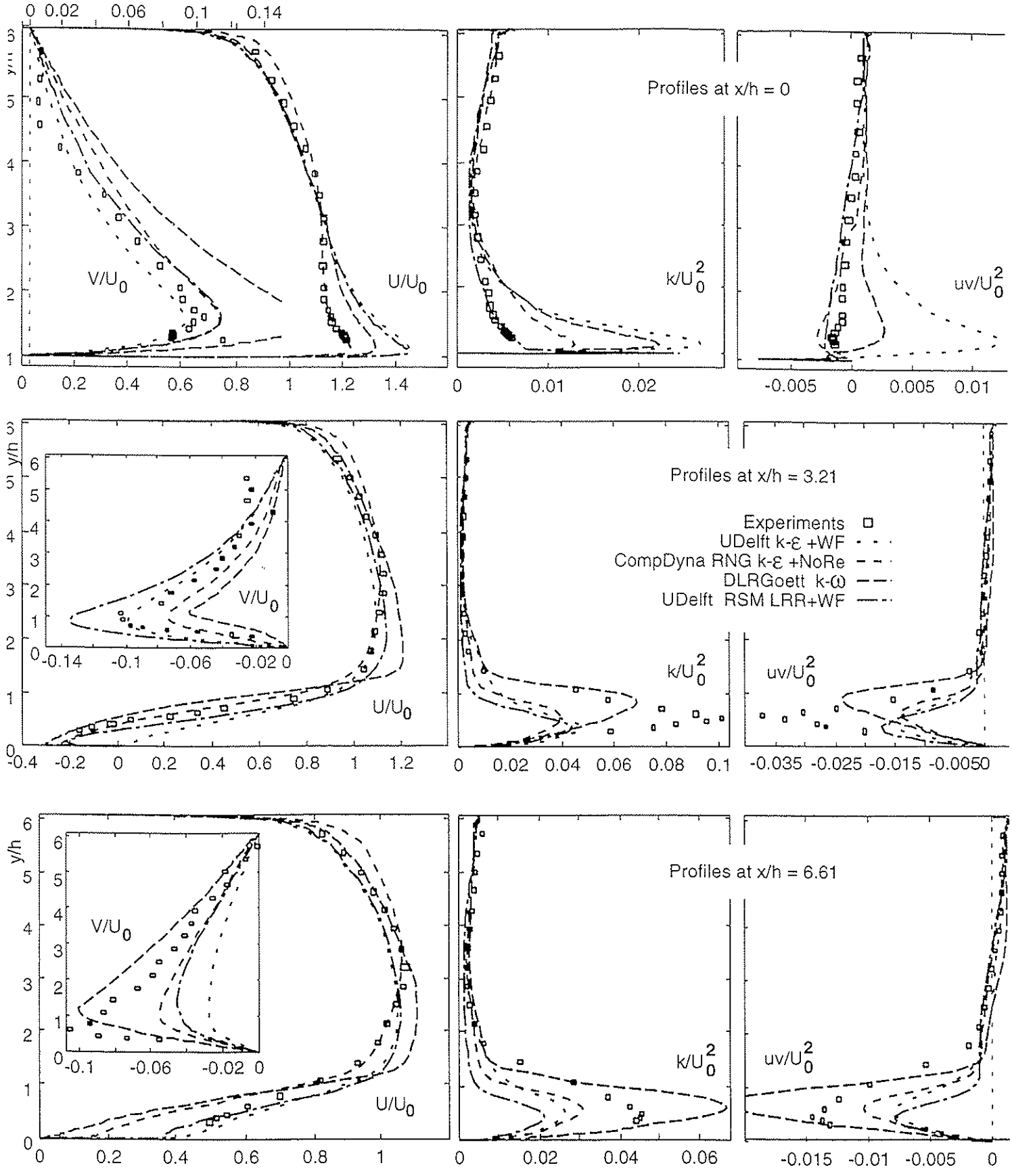

Fig. 7: Test case 2A: 2D single-hill flow; profiles at three x-locations

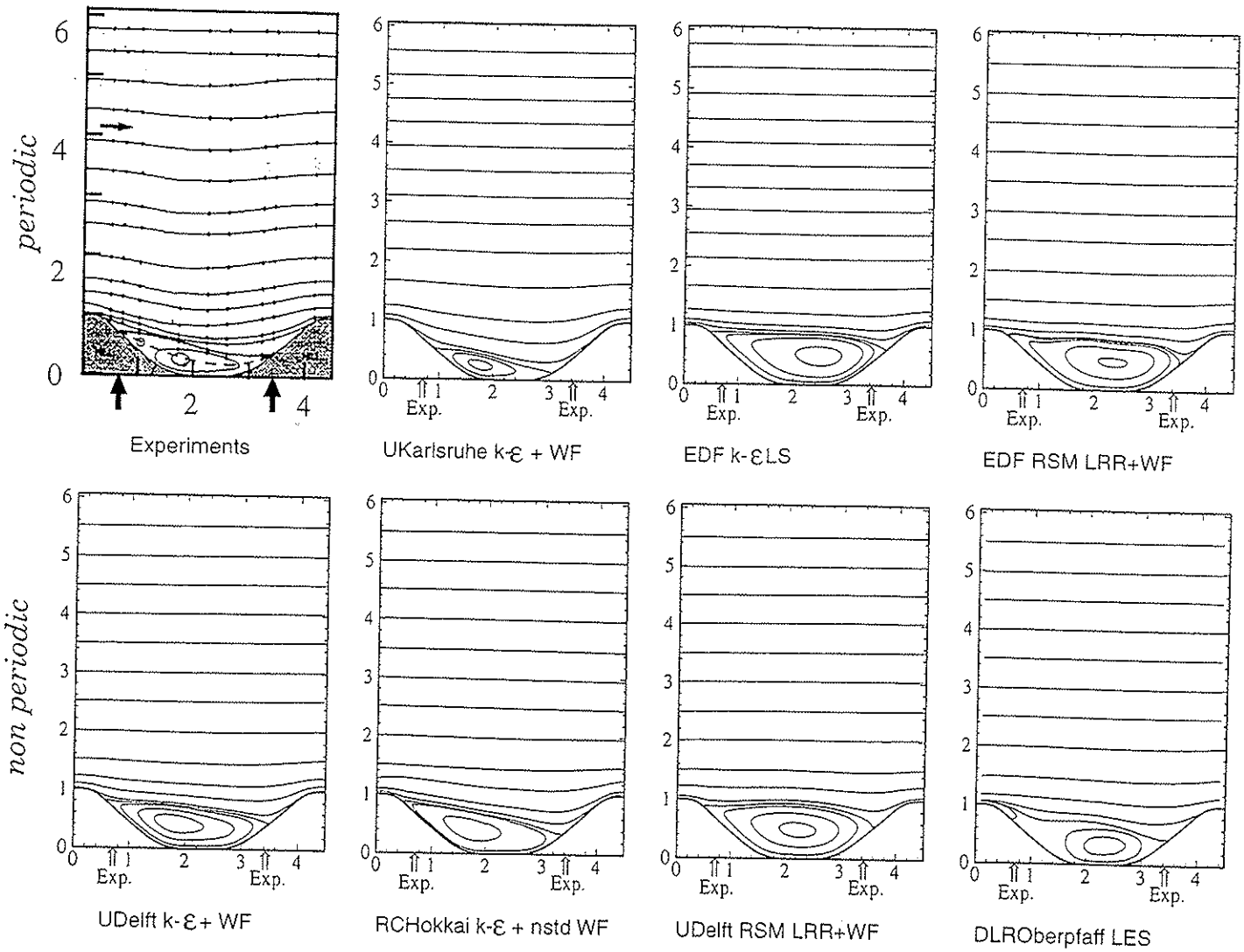

Fig. 8: Test case 2B: 2D periodic hill flow; streamlines

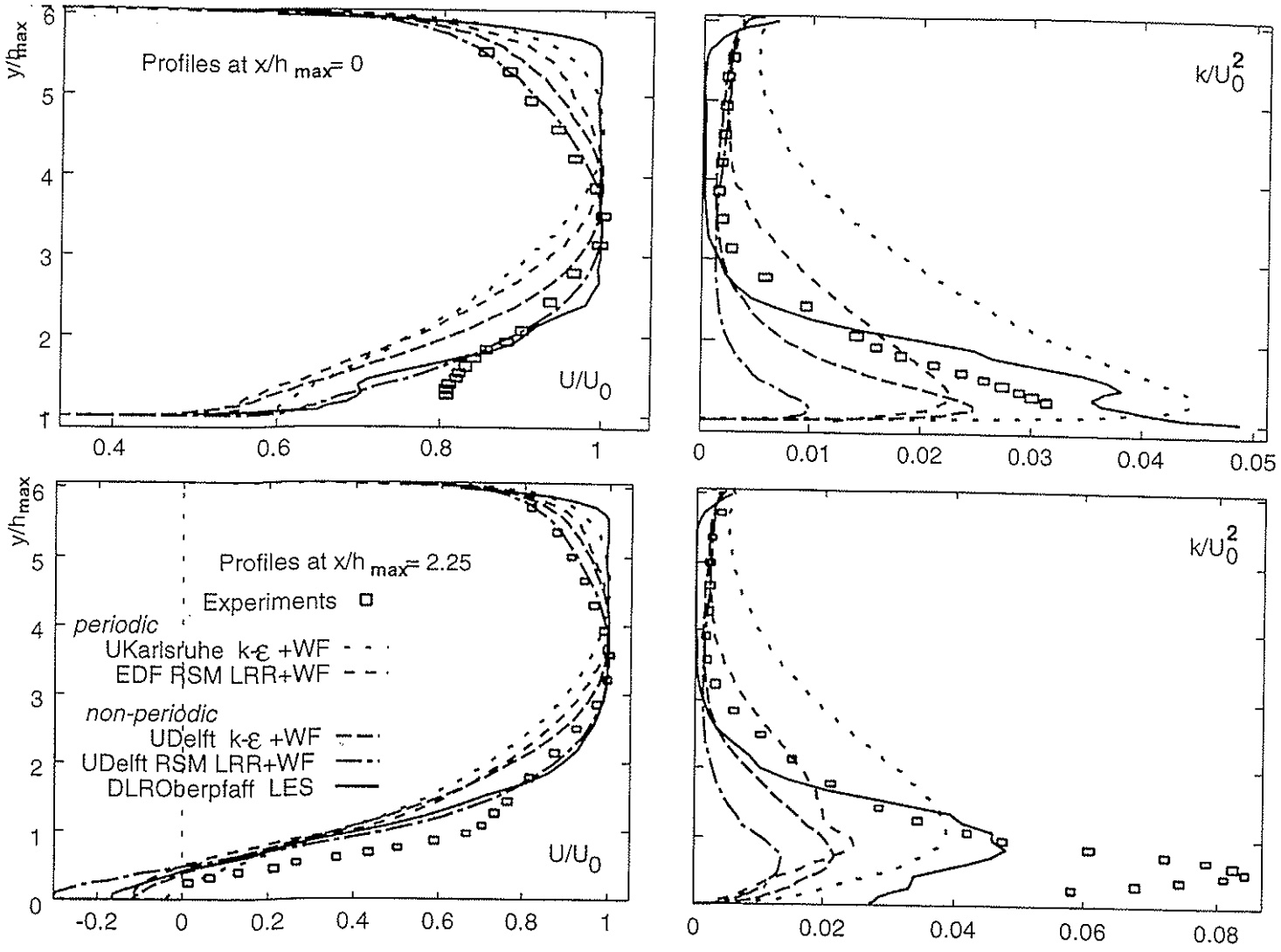

Fig. 9: Test case 2B: 2D periodic hill flow; profiles at two x-locations

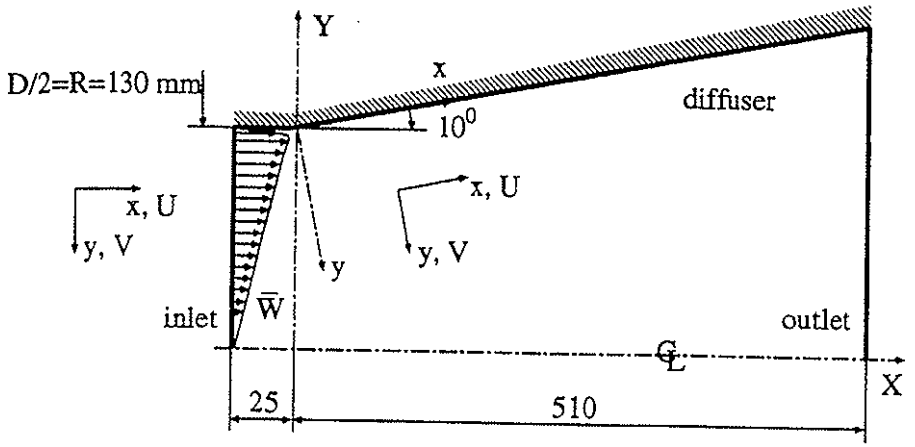

Fig. 10: Test case 3: Swirling boundary layer in conical diffuser; flow configuration

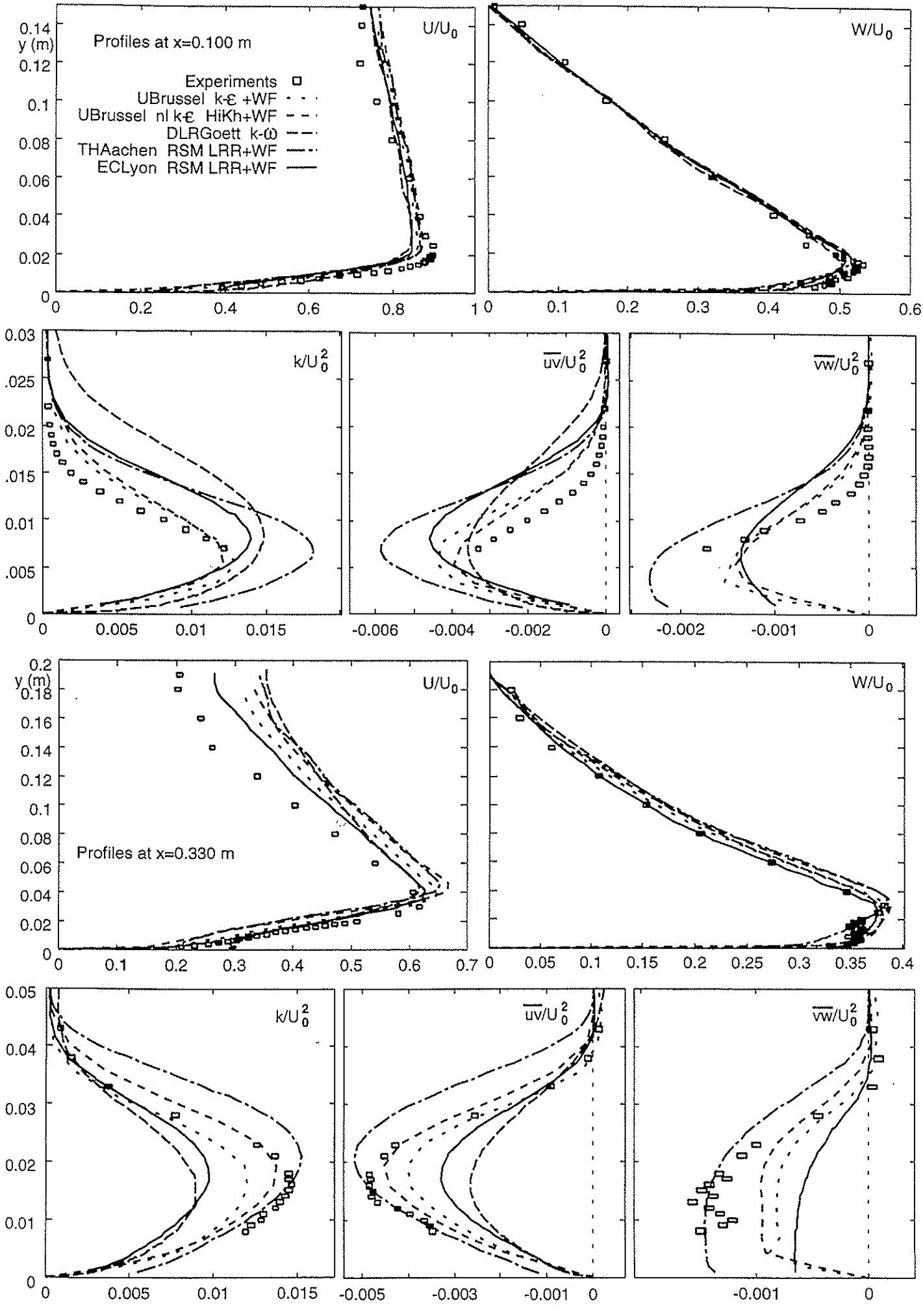

Fig. 11: Test case 3: Swirling boundary layer in conical diffuser; profiles at two x-locations

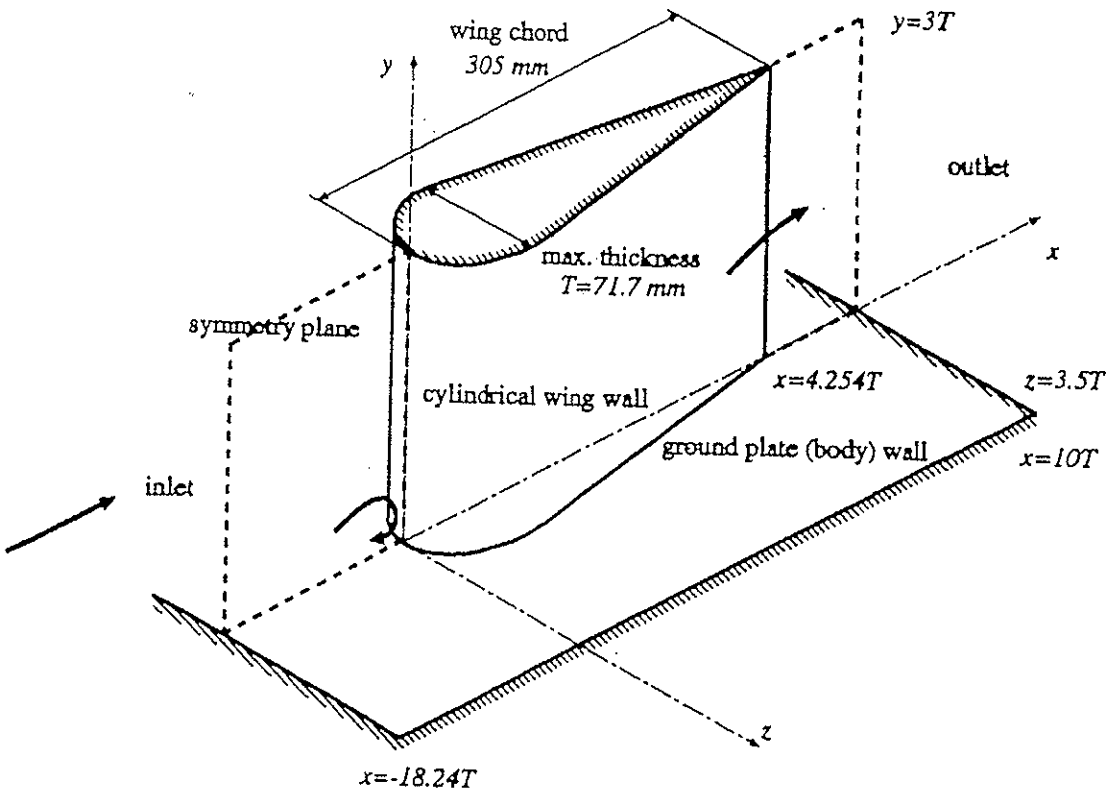

Fig. 12: Test case 4: Wing/body junction with separation; flow configuration

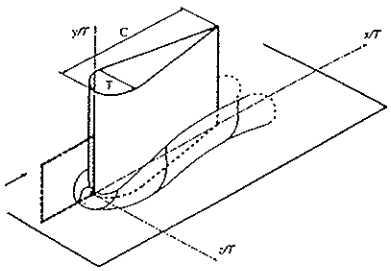

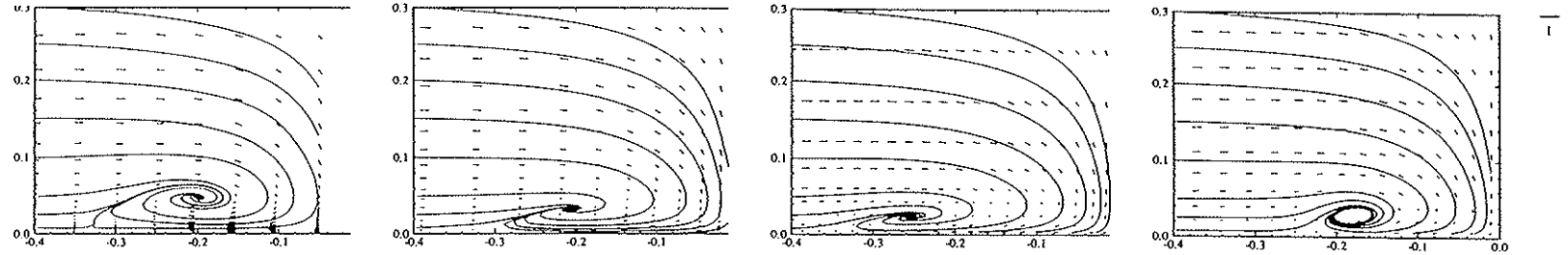

Experiments | ASC k-ε+ WF | CompDyna RNG k-ε+ WF | Volvo RSM LRR+WF

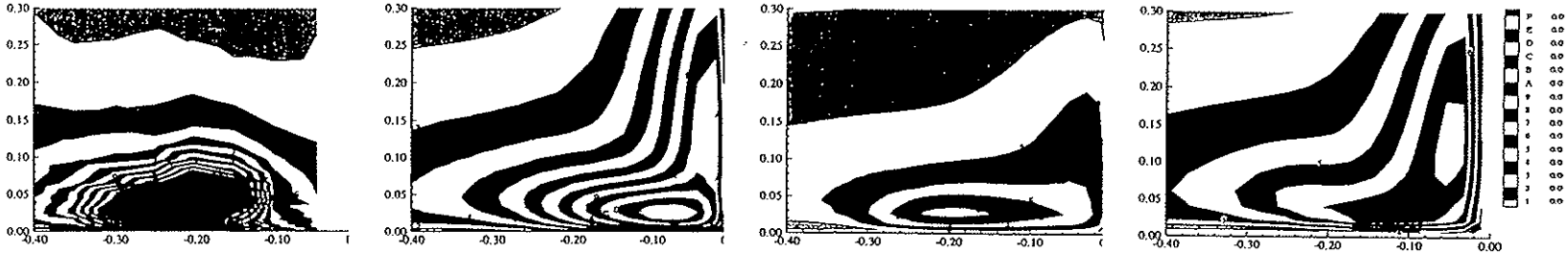

Experiments | ASC k-ε+ WF | CompDyna RNG k-ε+ WF | Volvo RSM LRR+WF

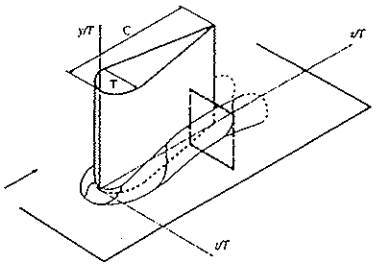

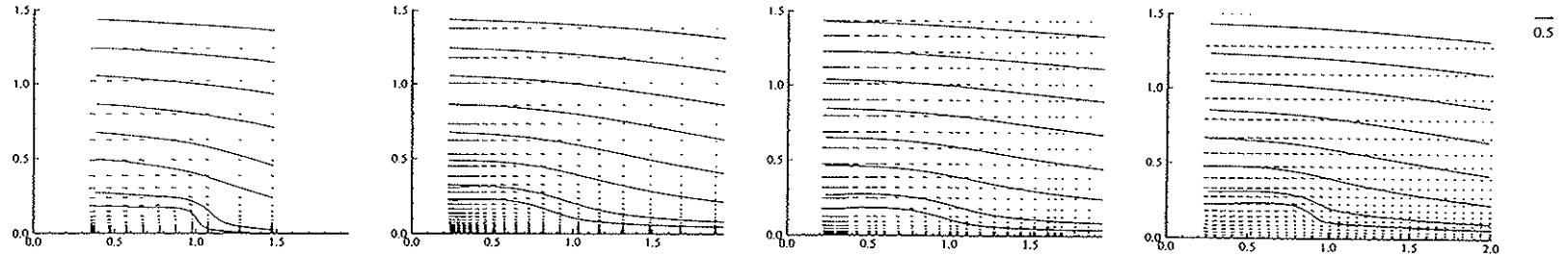

Experiments | ASC k-ε+ WF | CompDyna RNG k-ε+ WF | Volvo RSM LRR+WF

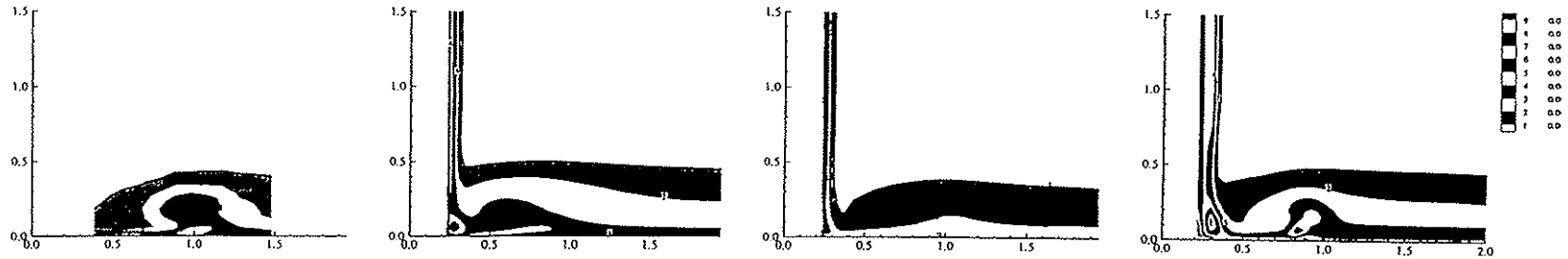

Experiments | ASC k-ε+ WF | CompDyna RNG k-ε+ WF | Volvo RSM LRR+WF

Fig. 13: Test case 4: Wing/body junction; secondary-flow velocity vectors and streamlines and k-contours in the two planes indicated in the sketches

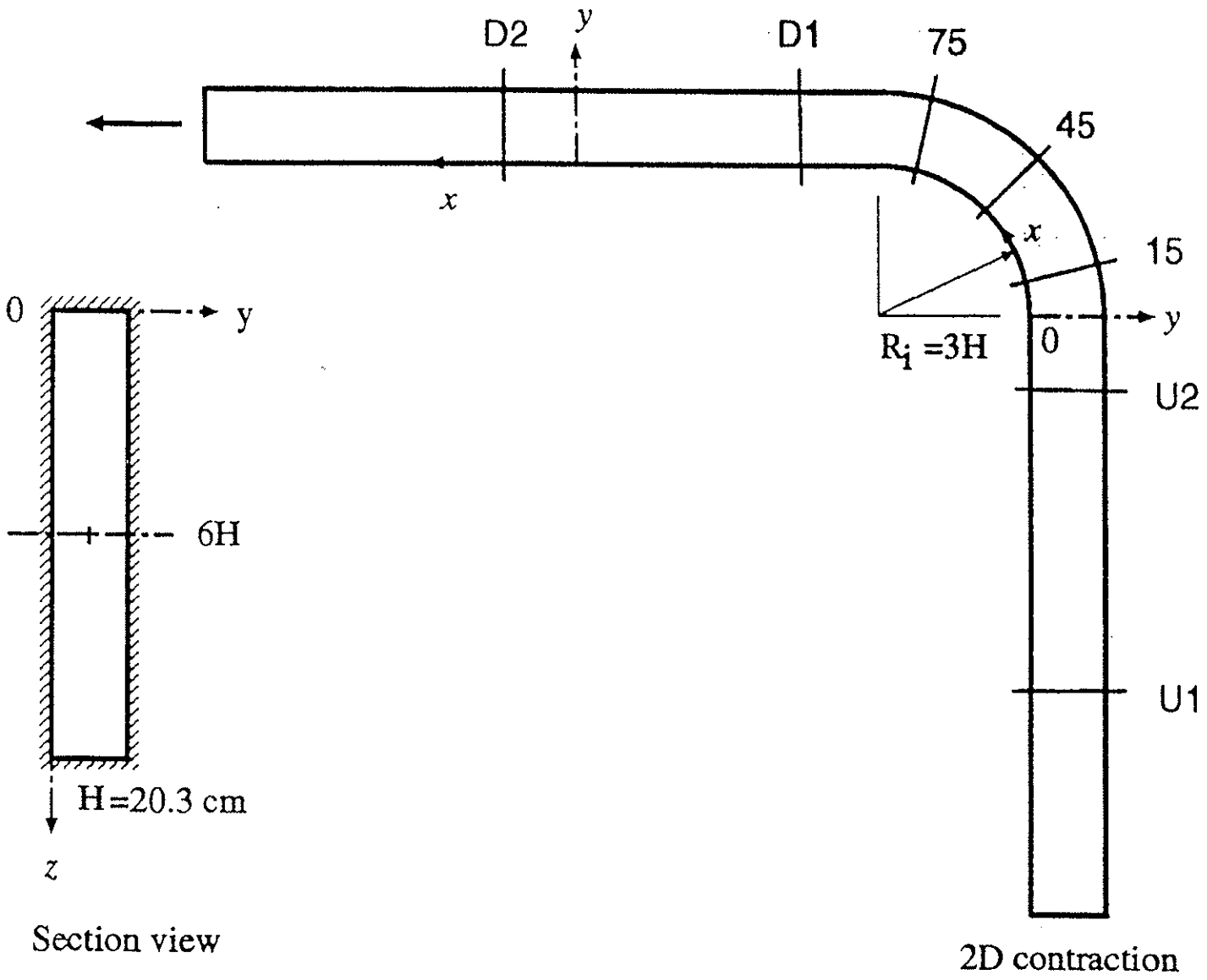

Fig. 14: Test case 5: Curved duct flow; flow configuration

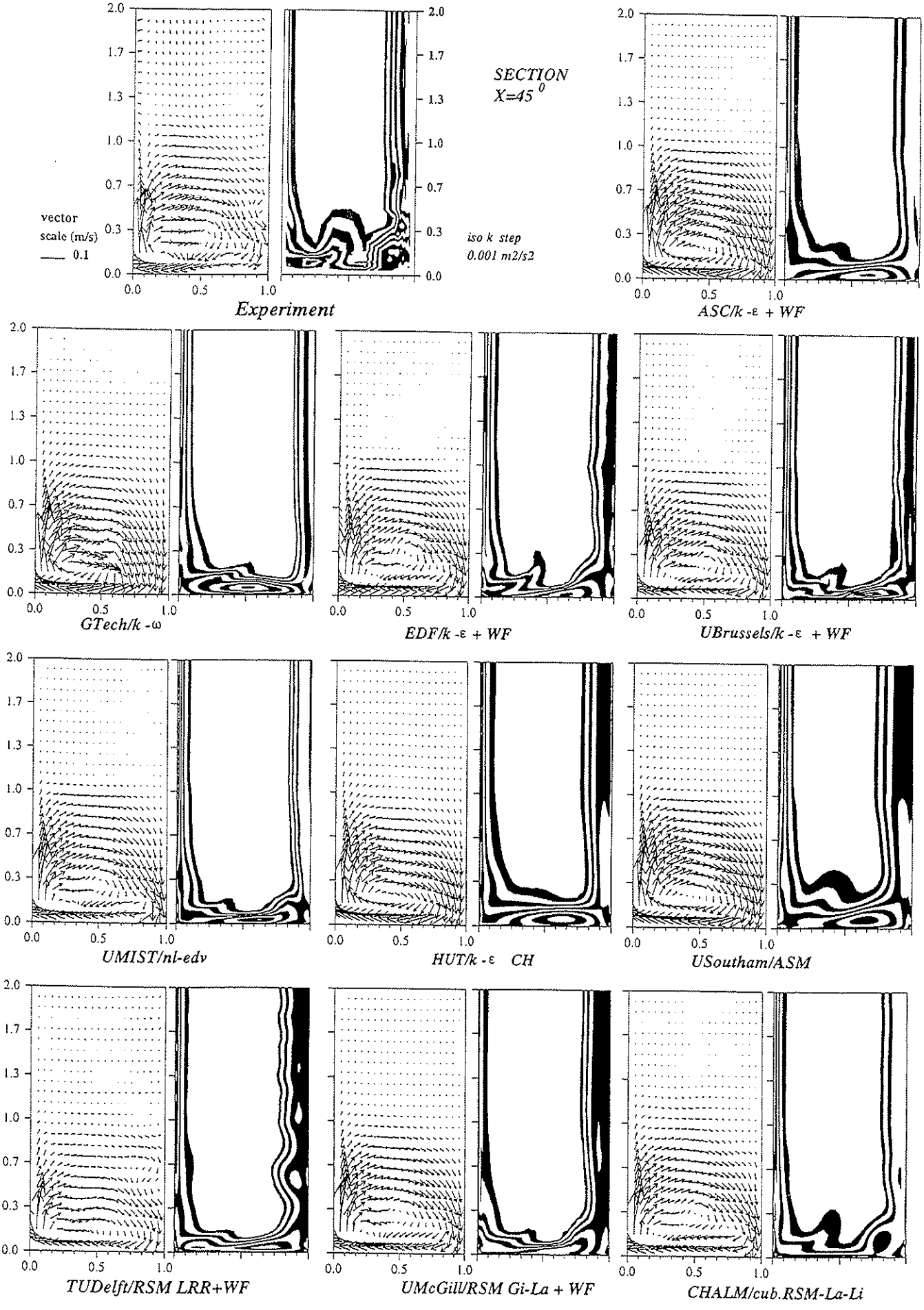

Fig. 15: Test case 5: Curved duct flow; secondary-flow velocity vectors and k-contours at 45°

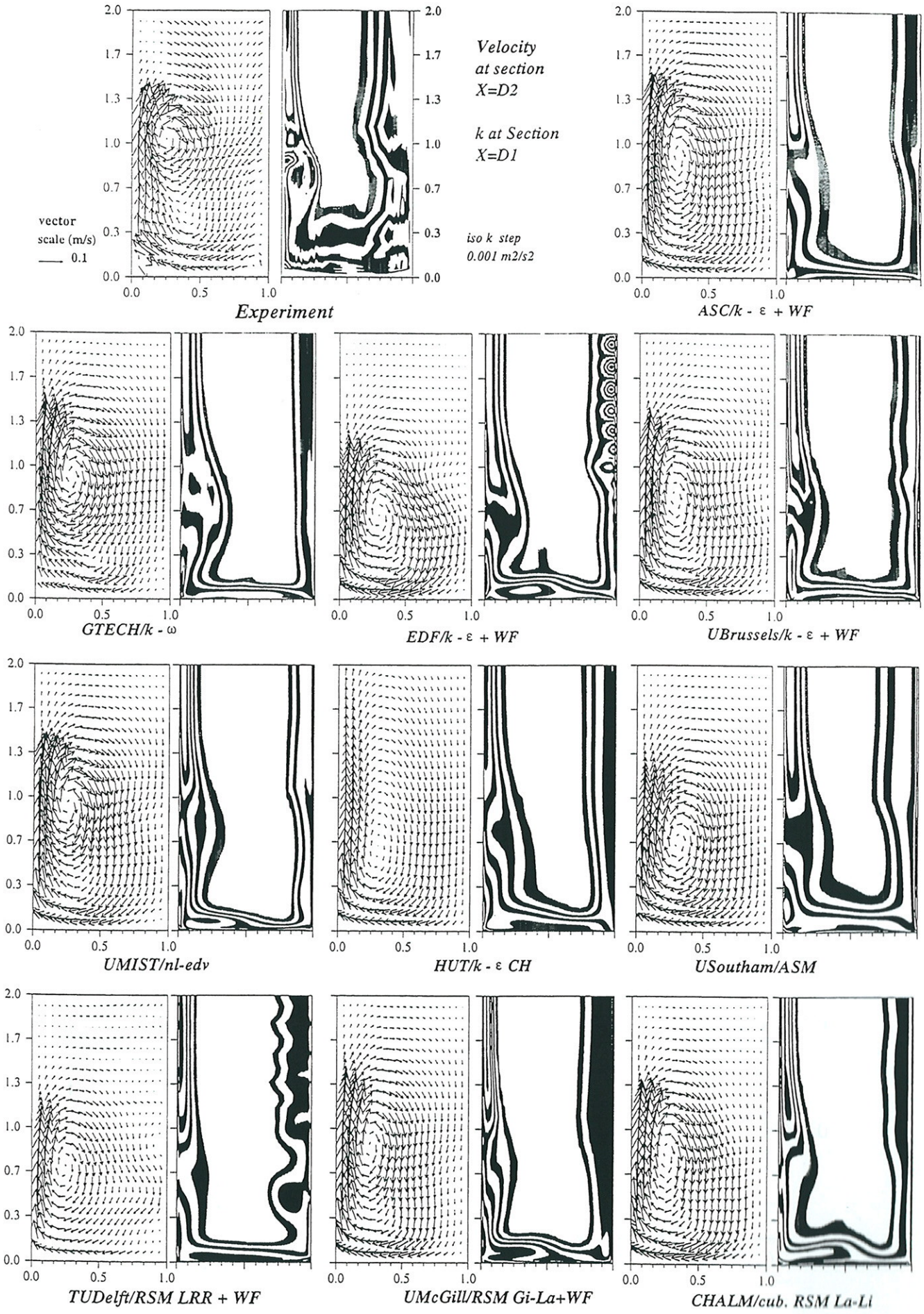

Fig. 16: Test case 5: Curved duct flow; secondary-flow vectors (at section D2) and k-contours (at section D1)

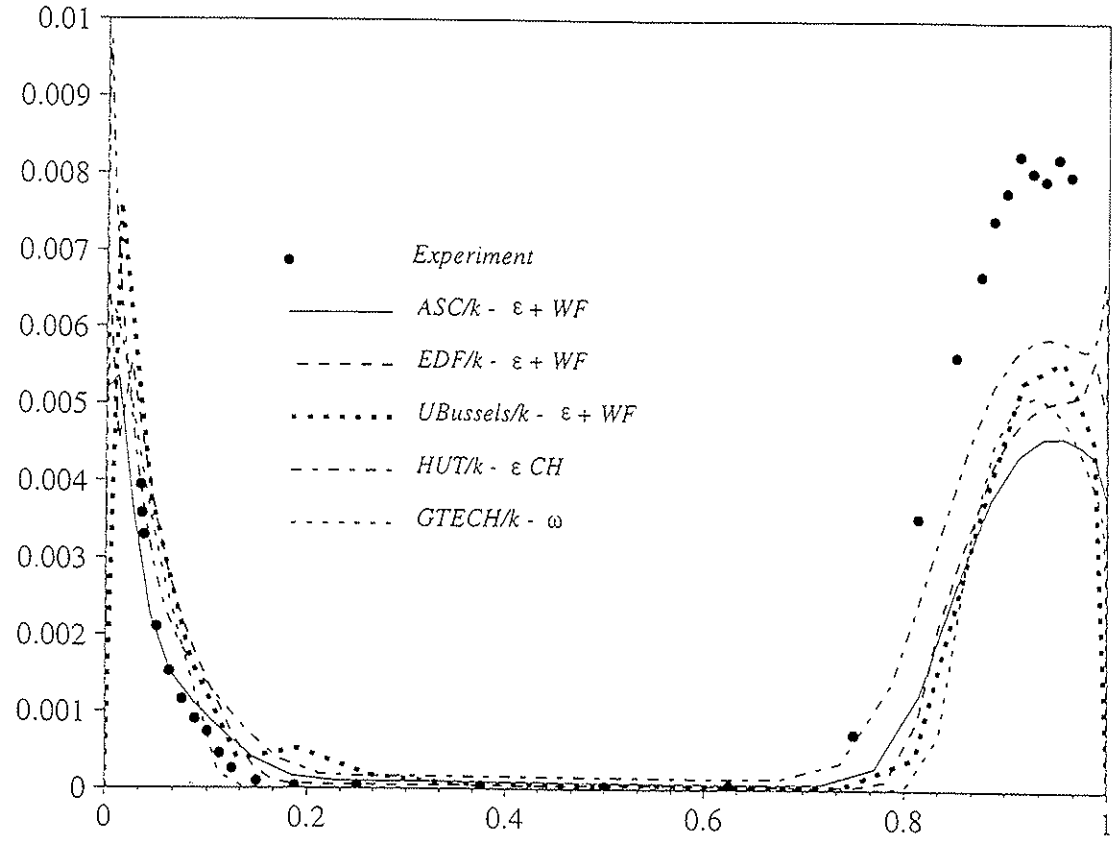

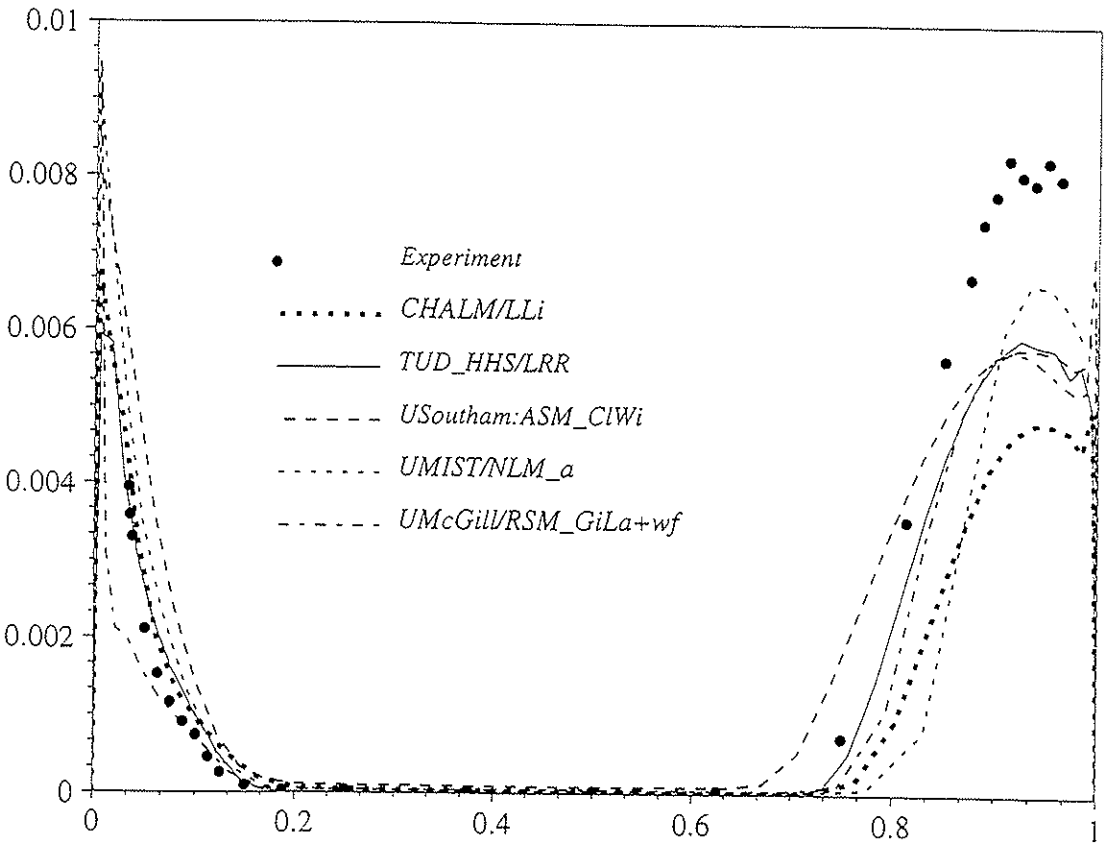

Fig. 17: Test case 5: Curved duct flow; k-profiles in symmetry plane (z = 3H) at 45°

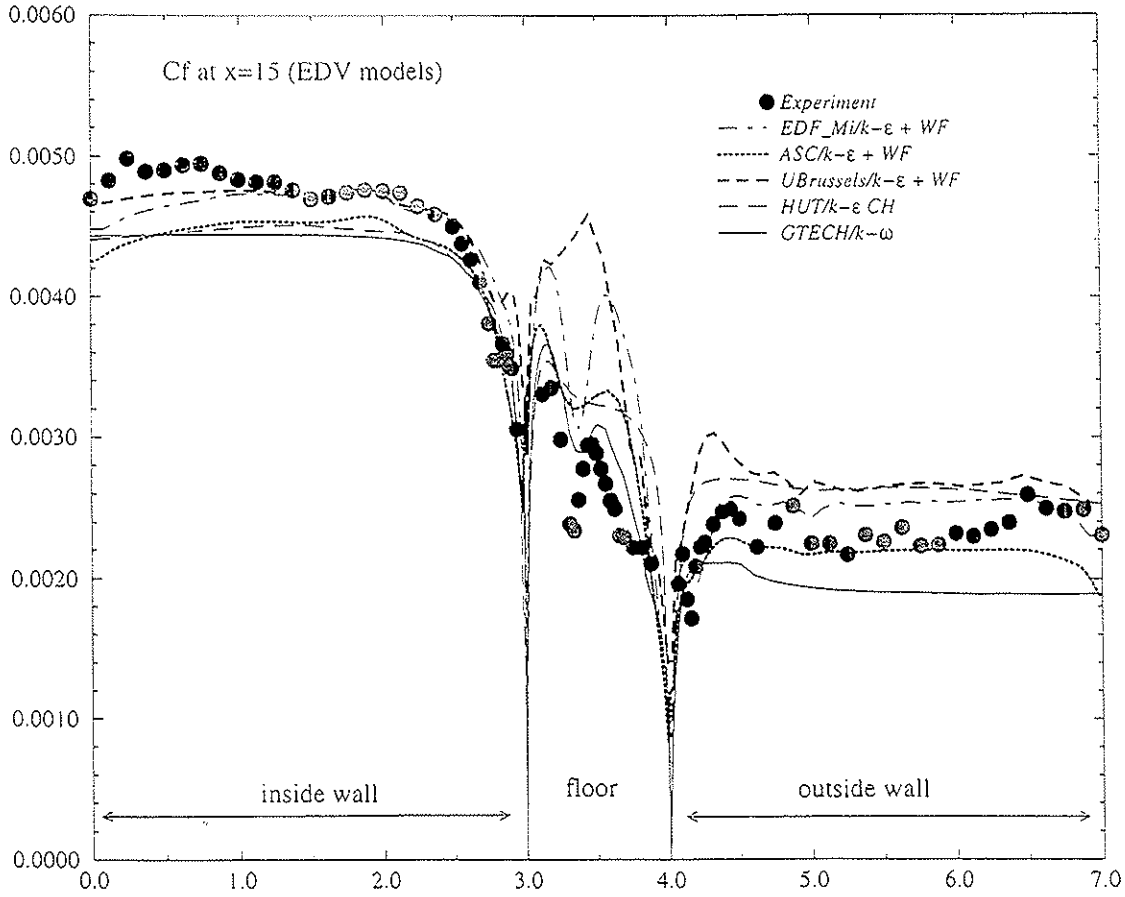

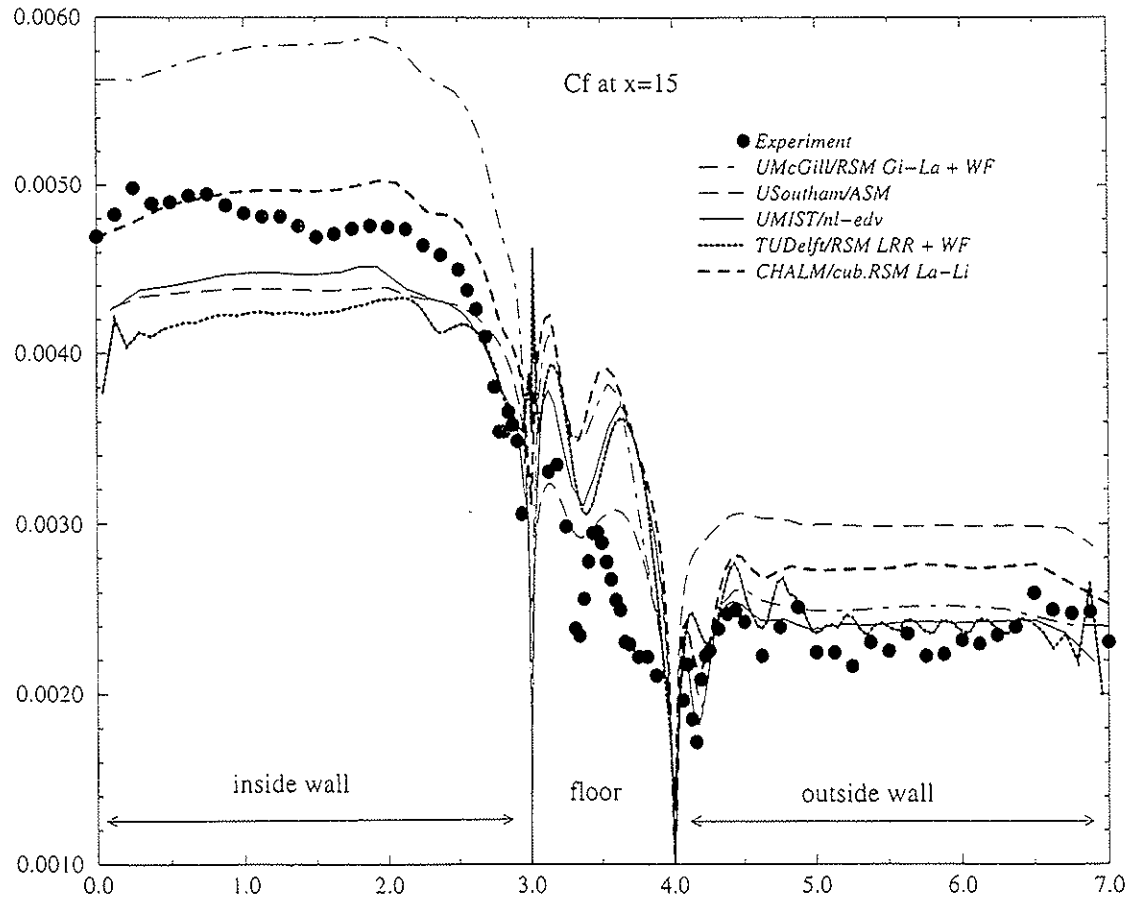

a) c_f-distribution at 15°

Fig. 18: Test case 5: Curved duct flow

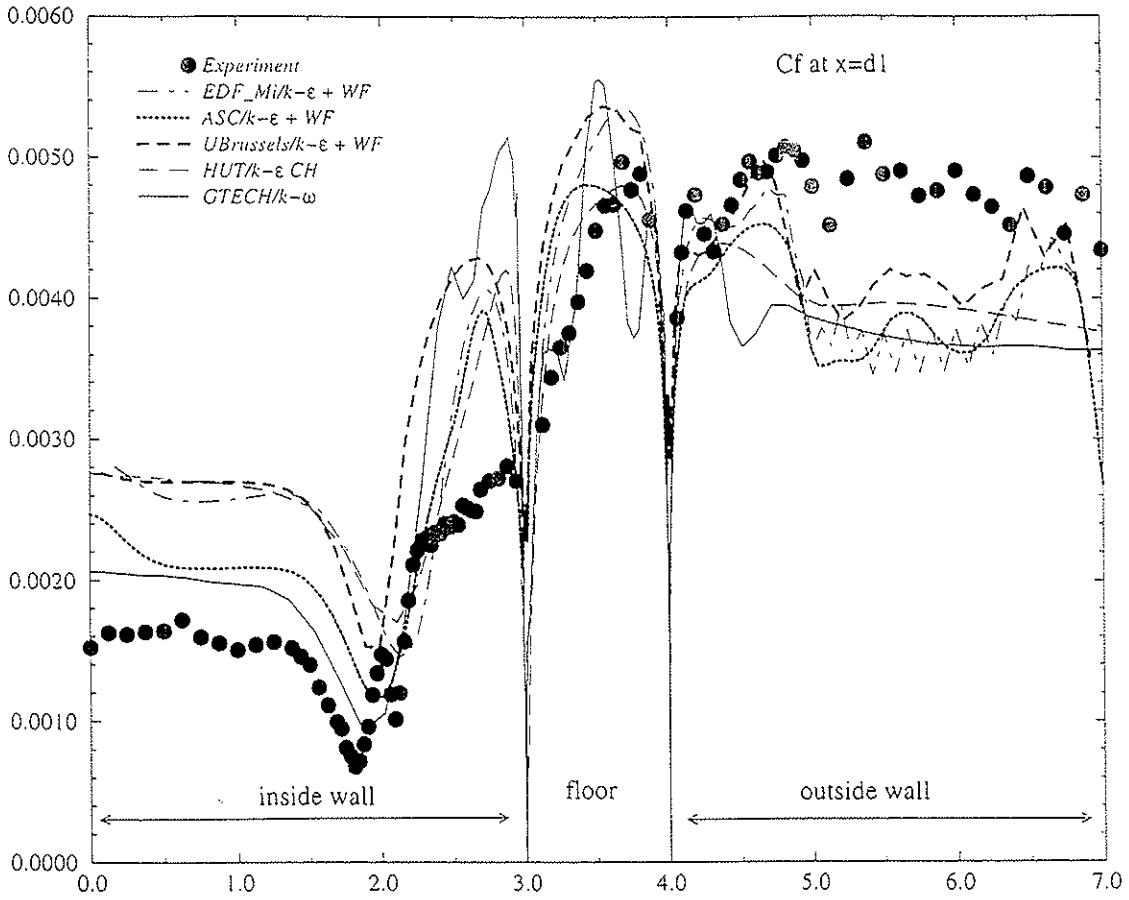

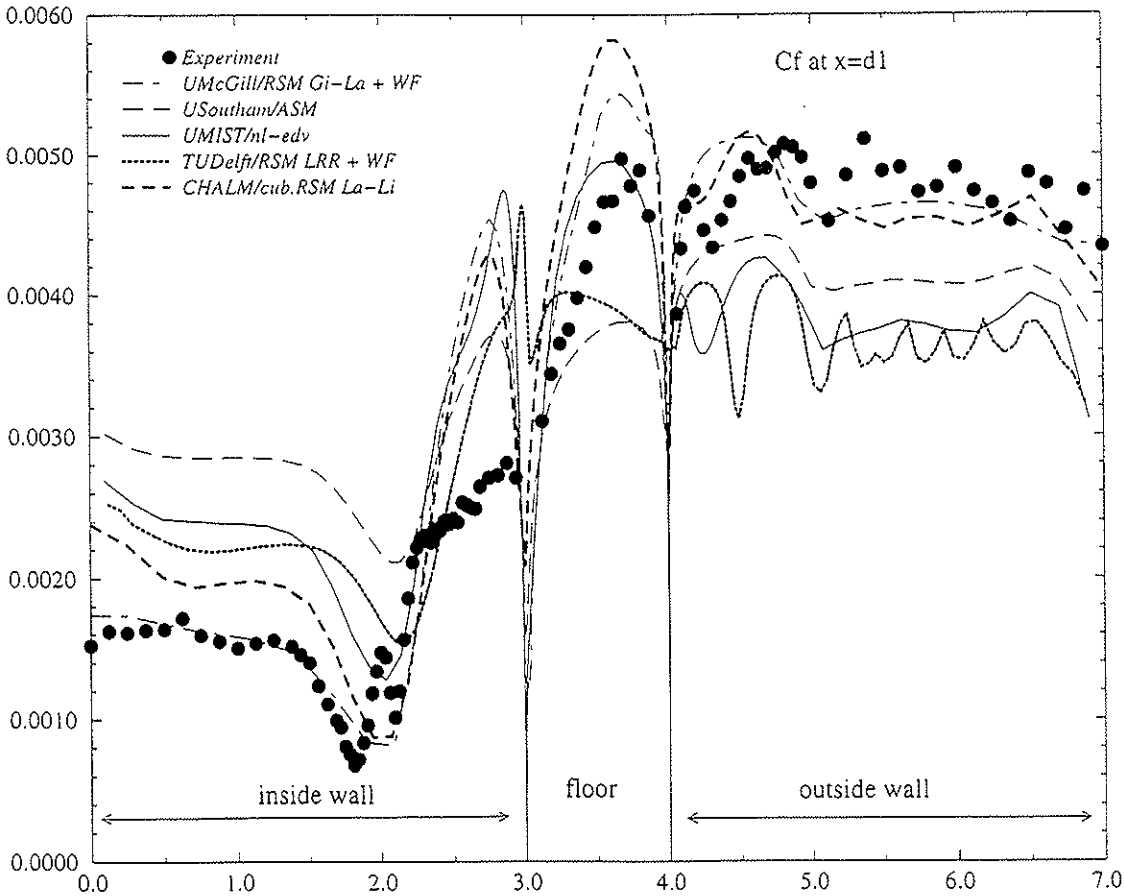

b) c_f-distribution at section D1

Fig. 18: Continued